Biochemical Pharmacology 89 (2014) 86–98

Contents lists available at ScienceDirect

Biochemical Pharmacology

journal homepage: www.elsevier.com/locate/biochempharm

Discovery of 3-(4-hydroxybenzyl)-1-(thiophen-2-yl)chromeno [2,3-c]pyrrol-9(2H)-one as a phosphodiesterase-5 inhibitor and its complex crystal structure☆

Na-Na Shang [a,1], Yong-Xian Shao [a,b,1], Ying-Hong Cai [a,1], Matthew Guan [b], Manna Huang [b], Wenjun Cui [b], Lin He [a], Yan-Jun Yu [a], Lei Huang [a], Zhe Li [a], Xian-Zhang Bu [a,*], Hengming Ke [a,b,*], Hai-Bin Luo [a,*]

[a] School of Pharmaceutical Sciences, Sun Yat-Sen University, Guangzhou 510006, PR China
[b] Department of Biochemistry and Biophysics and Lineberger Comprehensive Cancer Center, The University of North Carolina, Chapel Hill, NC 27599-7260, USA

ARTICLE INFO

Article history:
Received 31 December 2013
Accepted 14 February 2014
Available online 22 February 2014

Keywords:
Phosphodiesterase
Guanosine 3′,5′-cyclic monophosphate
PDE5 inhibitor
Crystal structure
Structure-based molecular design

ABSTRACT

Phosphodiesterase-5 (PDE5) inhibitors have been approved for the treatment of erectile dysfunction and pulmonary hypertension, but enthusiasm on discovery of PDE5 inhibitors continues for their potential new applications. Reported here is discovery of a series of new PDE5 inhibitors by structure-based design, molecular docking, chemical synthesis, and enzymatic characterization. The best compound, 3-(4-hydroxybenzyl)-1-(thiophen-2-yl)chromeno[2,3-c]pyrrol-9(2H)-one (**57**), has an IC_{50} of 17 nM against the PDE5 catalytic domain and good selectivity over other PDE families. The crystal structure of the PDE5 catalytic domain in complex with **57** was determined at 2 Å resolution and showed that **57** occupies the same pocket as other PDE5 inhibitors, but has a different binding pattern in detail. On the basis of the binding pattern of **57**, a novel scaffold can be proposed as a candidate of PDE inhibitors.

1. Introduction

Cyclic nucleotide phosphodiesterases (PDEs) are sole enzymes hydrolyzing cellular adenosine and guanosine 3′,5′-cyclic monophosphate (cAMP and cGMP) [1–3]. Cyclic AMP and cGMP are the second messengers mediating many physiological processes, including cardiac and smooth muscle contraction, steroid hormone function, adrenal hyperplasia, inflammation, axon guidance and regeneration, memory, and circadian regulation [4–8]. For the critical roles of cAMP and cGMP in cellular processes, PDE inhibitors have been widely studied as therapeutics for treatment of human diseases, such as diabetes, Alzheimer's disease, asthma, and erectile dysfunction [9–14].

The most successful examples of this drug class are the PDE5 inhibitors that have been approved for the treatment of several diseases: sildenafil (Viagra), vardenafil (Levetra), tadalafil (Cialis), avanafil (Stendra), udenafil (Zydena, Korean only), and mirodenafil (Mvix, Korean only) (Fig. 1) for erectile dysfunction [15–19]; sildenafil (Revatio) and tadalafil (Adcirca) for pulmonary arterial hypertension [9,20]; and tadalafil for benign prostatic hyperplasia [21]. In addition, preclinic and clinic trials have shown that PDE5 inhibitors are potent for treatment of many other human diseases, including lower urinary tract symptoms [22], benign prostatic hyperplasia [23], cardiovascular diseases [24–27], heart failure and coronary artery disease [28–30], second Raynaud's phenomenon [31], Duchenne muscular dystrophy [32], Peyronie's disease [33],

☆ *PDB Accession Codes*: The atomic coordinates and structure factors have been deposited into the RCSB Protein Data Bank with accession number 4MD6.
Chemical compounds studied in this article: *tert*-Butyl-2-(9-oxo-1-phenyl-2,9-dihydrochromeno[2,3-c]pyrrol-3-yl)acetate (ACP37; PubChem CID: 54770534); 3-Benzyl-1-phenylchromeno[2,3-c]pyrrol-9(2*H*)-one (ACP42; PubChem CID: 49784789); 3-(4-(*tert*-Butoxy)benzyl)-1-phenylchromeno[2,3-c]pyrrol-9(2*H*)-one (ACP43; PubChem CID: 54770536); 3-(9-Oxo-1-phenyl-2,9-dihydrochromeno[2,3-c]pyrrol-3-yl)propanoic acid (ACP52; PubChem CID: 72725677); 3-(4-Hydroxybenzyl)-1-(thiophen-2-yl)chromeno[2,3-c]pyrrol-9(2H)-one (ACP57; PubChem CID: 71765666); 3-(4-Hydroxybenzyl)-1-phenylchromeno[2,3-c]pyrrol-9(2H)-one (ACP61; PubChem CID: 71738344); 3-(4-Hydroxybenzyl)-2-methyl-1-phenylchromeno[2,3-c]pyrrol-9(2H)-one (ACP62; PubChem CID: 71738345).

* Corresponding authors.
E-mail addresses: phsbxzh@mail.sysu.edu.cn (X.-Z. Bu), hke@med.unc.edu (H. Ke), luohb77@mail.sysu.edu.cn (H.-B. Luo).
[1] These authors contribute equally to this work.

http://dx.doi.org/10.1016/j.bcp.2014.02.013
0006-2952/

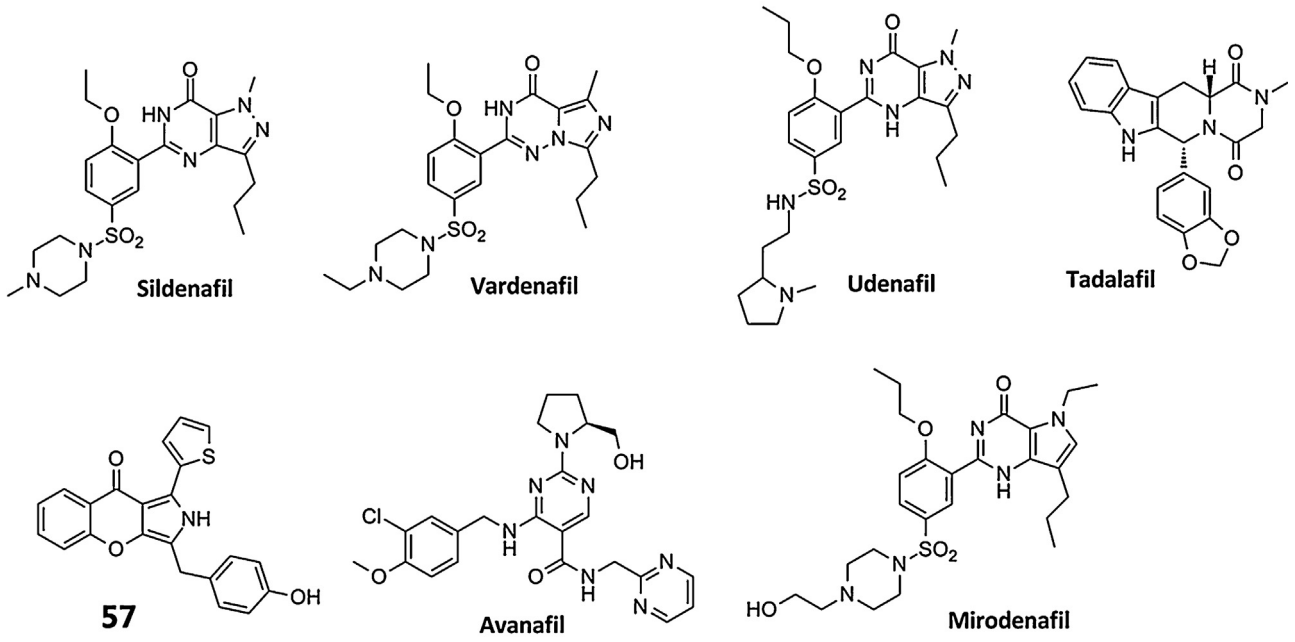

Fig. 1. Chemical structures of PDE5 inhibitors.

neurological disorders [34]. Moreover, PDE5 inhibitors have been used for anti-platelet therapy [35], wound healing [36], cognition enhancement [37], and improvement of sperm quality [38]. However, PDE5 inhibitors have been shown to have some adverse side effects such as vision disturbance [39] and hearing loss [40]. Thus, study of PDE5 inhibitors still attracts great attention of both academic and industrial researchers, to discover new compounds that may have potential new applications and also less severe side effects.

Reported in this paper are the structure-based design, chemical synthesis, and structural and enzymatic characterization of the PDE5 inhibitors. The best compound 3-(4-hydroxybenzyl)-1-(thiophen-2-yl)chromeno[2,3-c]pyrrol-9(2H)-one (**57**) exhibits strong inhibitory affinity (IC_{50} = 17 nM) against PDE5 and good selectivity over other PDE families. The crystal structure of the PDE5A1 catalytic domain in complex with **57** was solved and the molecular docking suggested a novel scaffold that may be used as a molecular core for development of new PDE5 inhibitors.

2. Materials and methods

2.1. Reagents and synthesis

All reagents used were commercially available. Amino acids, DMAP (dimethylaminopyridine) and DCC (dicyclohexylcarbodiimide) were bought from GL Biochem (Shanghai) Ltd. Acetophenones, aryl chlorides and all other chemicals were bought from Alfa Aesar (Tianjin) chemical Ltd. Amino acids were treated as follows: α-amino groups were protected with Fmoc (9-fluorenylmethoxycarbonyl), the side chains of lysine and tryptophan were protected with Boc (*tert*-butyloxy carbonyl), and the side chains of aspartic acid, glutamic acid and tyrosine were protected as ^{t}Bu (*tert*-butyl). Reactions were monitored by thin layer chromatography (TLC) on a glass plate coated with silica gel with fluorescent indicator (GF_{254}). Column chromatography was performed on silica gel (200–300 mesh). ^{1}H NMR and ^{13}C NMR spectra were recorded using TMS as an internal standard with a Burker BioSpin Ultrashield 400 NMR system at 400 MHz and 100 MHz, respectively. The purity of targeted compounds was determined on a DIONEX Ultimate 3000 HPLC System (Chromeleon SR9 Build 2673); column, Acclaim® 120 C_{18}, 5 μm, 4.6 × 250 mm; mobile phase, solvent A: water, solvent B: CH_3CN, flow rate, 1 ml/min; UV wavelength, 254 nm; temperature, ambient. The linear gradient procedure was used to purify the compounds: 65%–99% B for **16**–**26**, **33**–**49**, and **60**; 40% B + 1/1000 TFA to 80% B for **50**, **52**, **54**, and **56**; 45% to 95% B for **51**, **53**, **55**, **57**–**59**, **61**, and **62**. Most compounds have purity >95%, as calculated with the percentage peak area of the analyzed compounds in the HPLC system. High resolution mass spectra (HRMS) were recorded on Shimadzu LCMS-IT-TOF.

The syntheses of the new compounds **16**–**26**, **33**–**36**, **38**–**40**, and **48**–**62** are diagramed in Scheme 1 and described as follows. Compounds **37**, **41**–**47** were previously reported [41].

2.1.1. 1-(2-Hydroxyphenyl)-3-phenylpropane-1,3-dione (*1*)

1.36 g 2-Hydroxyacetophenone (10 mmol) and 2.1 g benzoyl chloride (15 mmol) were dissolved in pyridine (25 mL) with stir at 25 °C. When 2-hydroxyacetophenone was consumed as determined by using TLC in about 4–5 h, excess of water was added and the pH of the mixture was adjusted to 5.0 with 10% HCl. The precipitated product was collected by filtration, giving the ester intermediate in the form of white powder. The crude product was dissolved in 50 mL pyridine and 1–1.5*eq* KOH was added. After the mixture was heated to 60 °C for 6–8 h, excess of water was added and the pH of the solution was adjusted to 5.0 with 10% HCl. The product was precipitated and collected by filtration. The yellow powder was purified by recrystallization with alcohol to afford 1.99 g product **1**, yield 83%; ^{1}HNMR (400 MHz, $CDCl_3$), δ 15.53 (1H), 12.08 (1H), 7.93 (d, *J* = 7.5 Hz, 2H), 7.77 (d, *J* = 8.0 Hz, 1H), 7.55 (t, *J* = 7.3 Hz, 1H), 7.47 (dd, *J* = 16.5, 8.1 Hz, 3H), 7.00 (d, *J* = 8.4 Hz, 1H), 6.92 (t, *J* = 7.6 Hz, 1H), 6.83 (1H).

2.1.2. 1-(Furan-2-yl)-3-(2-hydroxyphenyl)propane-1,3-dione (*2*)

1.36 g 2-Hydroxyacetophenone (10 mmol) and 1.95 g furan-2-carbonyl chloride (15 mmol) were treated by the procedure used for the synthesis of **1**, giving 2.07 g **2** as yellow crystal, yield 90%; ^{1}H NMR (400 MHz, $CDCl_3$), δ 15.09 (1H), 12.08 (1H), 7.78 (d, *J* = 8.1 Hz, 1H), 7.62 (s,1H), 7.47 (dd, *J* = 8.2, 7.3 Hz, 1H), 7.19 (d, *J* = 3.5 Hz, 1H), 7.00 (d, *J* = 8.4 Hz, 1H), 6.93 (dd, *J* = 8.0, 7.2 Hz, 1H), 6.79 (s,1H), 6.61–6.59 (m, 1H).

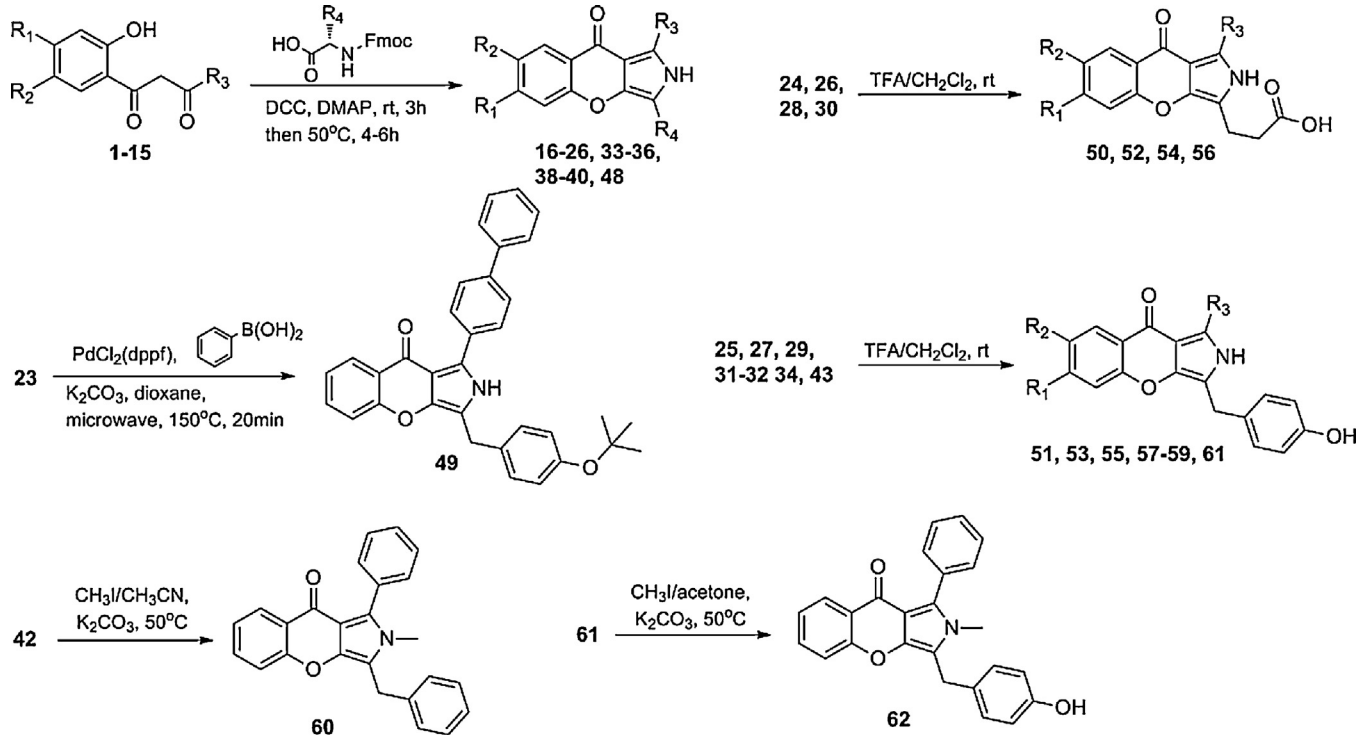

Scheme 1. Syntheses of **16**–**26**, **33**–**36**, **38**–**40**, **48**–**62.** Only the non-H groups are described as follows. **16**: $R_2 = CH_3$, R_3 = furan-2-yl, $R_4 = CH_2COO^tBu$; **17**: $R_2 = OCH_3$, R_3 = furan-2-yl, $R_4 = CH_2CH_2COO^tBu$; **18**: $R_2 = CH_3$, R_3 = furan-2-yl, $R_4 = CH_2CH_2COO^tBu$; **19**: $R_2 = CH_3$, R_3 = furan-2-yl, $R_4 = CH_2C_6H_4(p\text{-}O^tBu)$; **20**: R_3 = furan-2-yl, $R_4 = CH_2C_6H_4(p\text{-}O^tBu)$; **21**: R_3 = furan-2-yl, $R_4 = CH_2CH_2COO^tBu$; **22**: $R_2 = Br$, R_3 = furan-2-yl, $R_4 = CH_2CH_2COO^tBu$; **23**: R_3 = 4-Br-C_6H_4, $R_4 = CH_2C_6H_4(p\text{-}O^tBu)$; **24**: $R_2 = OCH_3$, R_3 = thiophen-2-yl, $R_4 = CH_2CH_2COO^tBu$; **25**: $R_2 = OCH_3$, R_3 = thiophen-2-yl, $R_4 = CH_2C_6H_4(p\text{-}O^tBu)$; **26**: $R_3 = C_6H_5$, $R_4 = CH_2CH_2COO^tBu$; **33**: R_3 = naphthalen-2-yl, $R_4 = CH_2C_6H_5$; **34**: R_3 = naphthalen-2-yl, $R_4 = CH_2C_6H_4(p\text{-}O^tBu)$; **35**: $R_2 = OCH_3$, R_3 = thiophen-2-yl, $R_4 = CH_2COO^tBu$; **36**: R_3 = 4-Br-C_6H_4, $R_4 = CH_2C_6H_5$; **38**: R_3 = 4-F-C_6H_4, $R_4 = CH_2COO^tBu$; **39**: $R_2 = CH_3$, R_3 = 4-F-C_6H_4, $R_4 = CH_2COO^tBu$; **40**: R_3 = 4-F-C_6H_4, R_4 = N-Boc-*1H*-indol-3-yl; **48**: $R_2 = OCH_3$, R_3 = thiophen-2-yl, $R_4 = CH_2(CH_2)_3NHCOO^tBu$; **50**: $R_2 = OCH_3$, R_3 = thiophen-2-yl; **51**: $R_2 = OCH_3$, R_3 = thiophen-2-yl; **52**: $R_3 = C_6H_5$; **53**: $R_2 = CH_3$, R_3 = 4-F-C_6H_4; **54**: $R_2 = Br$, R_3 = thiophen-2-yl; **55**: $R_2 = Br$, R_3 = thiophen-2-yl; **56**: $R_2 = CH_3$, R_3 = 4-F-C_6H_4; **57**: R_3 = thiophen-2-yl; **58**: R_3 = 4-OCH_3-C_6H_4; **59**: R_3 = naphthalen-2-yl; **61**: $R_3 = C_6H_5$.

*2.1.3. 1-(Furan-2-yl)-3-(2-hydroxy-5-methylphenyl)propane-1,3-dione (**3**)*

1.5 g 1-(2-Hydroxy-5-methylphenyl)ethanone (10 mmol) and 1.95 g furan-2-carbonyl chloride (15 mmol) were treated by the procedure used for the synthesis of **1**, giving 1.83 g **3** as yellow powder, yield 75%; ^{1}H NMR (400 MHz, $CDCl_3$), δ 15.17 (1H), 11.89 (1H), 7.64 (dd, J = 1.6, 0.7 Hz, 1H), 7.55 (1H), 7.31–7.28 (m, 1H), 7.20–7.18 (m, 1H), 6.91 (d, J = 8.5 Hz, 1H), 6.78 (1H), 6.62 (dd, J = 3.5, 1.7 Hz, 1H), 2.35 (3H).

*2.1.4. 1-(5-Bromo-2-hydroxyphenyl)-3-(furan-2-yl)propane-1,3-dione (**4**)*

2.15 g 1-(5-Bromo-2-hydroxyphenyl)ethanone (10 mmol) and 1.95 g furan-2-carbonyl chloride (15 mmol) were treated by the procedure used for the synthesis of **1**, giving 2.84 g **4** as yellow powder, yield 92%; ^{1}H NMR (400 MHz, $CDCl_3$) δ 14.98 (1H), 12.02 (1H), 7.85 (s,1H), 7.65 (s,1H), 7.52 (d, J = 8.9 Hz, 1H), 7.21 (d, J = 3.0 Hz, 1H), 6.90 (d, J = 8.3 Hz, 1H), 6.70 (s,1H), 6.63–6.60 (m, 1H).

*2.1.5. 1-(5-Bromo-2-hydroxyphenyl)-3-(thiophen-2-yl)propane-1,3-dione (**5**)*

2.15 g 1-(5-Bromo-2-hydroxyphenyl)ethanone (10 mmol) and 2.19 g thiophene-2-carbonylchloride (15 mmol) were treated by the procedure used for the synthesis of **1**, giving 3.12 g **5** as yellow powder, yield 96%; ^{1}H NMR (400 MHz, $CDCl_3$) δ 15.59 (1H), 11.91 (1H), 7.85–7.83 (m, 1H), 7.81 (d, J = 2.4 Hz, 1H), 7.65 (d, J = 4.9 Hz, 1H), 7.52 (dd, J = 8.9, 2.4 Hz, 1H), 7.21–7.18 (m, 1H), 6.91 (dd, J = 8.9, 3.0 Hz, 1H), 6.61 (s,1H).

*2.1.6. 1-(4-Fluorophenyl)-3-(2-hydroxyphenyl)propane-1,3-dione (**6**)*

1.36 g 2-Hydroxyacetophenone (10 mmol) and 2.37 g 4-fluorinebenzoyl chloride (15 mmol) were treated by the procedure used for the synthesis of **1**, giving 2.2 g **6** as yellow crystal, yield 86%; ^{1}H NMR (400 MHz, $CDCl_3$) δ 15.60 (1H), 12.02 (1H), 7.98–7.91 (m, 2H), 7.76 (d, J = 8.1 Hz, 1H), 7.47 (dd, J = 8.3, 7.2 Hz, 1H), 7.18 (dd, J = 12.4, 4.9 Hz, 2H), 7.00 (d, J = 8.4 Hz, 1H), 6.92 (t, J = 7.6 Hz, 1H), 6.78 (1H).

*2.1.7. 1-(4-Fluorophenyl)-3-(2-hydroxy-5-methylphenyl)propane-1,3-dione (**7**)*

1.5 g 1-(2-Hydroxy-5-methylphenyl)ethanone (10 mmol) and 2.37 g 4-fluorinebenzoyl chloride (15 mmol) were treated by the procedure used for the synthesis of **1**, giving 2.36 g **7** as yellow powder, yield 87%; ^{1}H NMR (400 MHz, $CDCl_3$) δ 15.68 (1H), 11.83 (1H), 8.00–7.94 (m, 2H), 7.53 (s,1H),7.29 (d, J = 8.5 Hz, 1H), 7.18 (dd, J = 12.0, 5.2 Hz, 2H), 6.91 (d, J = 8.5 Hz, 1H),6.77 (s,1H), 2.34 (3H).

*2.1.8. 1-(Furan-2-yl)-3-(2-hydroxy-5-methoxyphenyl)propane-1,3-dione (**8**)*

1.66 g 1-(2-Hydroxy-5-methoxyphenyl)ethanone (10 mmol) and 1.95 g furan-2-carbonyl chloride (15 mmol,) were treated by the procedure used for the synthesis of **1**, giving 2.36 g **8** as yellow powder, yield 91%; ^{1}H NMR (400 MHz, $CDCl_3$) δ 15.19 (s, 1H), 11.64 (s, 1H), 7.62 (d, J = 0.9 Hz, 1H), 7.20 (d, J = 3.0 Hz, 1H), 7.19 (dd, J = 3.5, 0.5 Hz, 1H), 7.10 (dd, J = 9.0, 3.0 Hz, 1H), 6.94 (d, J = 9.0 Hz, 1H), 6.72 (s, 1H), 6.61 (dd, J = 3.5, 1.7 Hz, 1H), 3.84 (s, 3H).

*2.1.9. 1-(2-Hydroxy-5-methoxyphenyl)-3-(thiophen-2-yl)propane-1,3-dione (**9**)*

1.66 g 1-(2-Hydroxy-5-methoxyphenyl)ethanone (10 mmol) and 2.19 g thiophene-2-carbonyl chloride (15 mmol) were treated by the procedure used for the synthesis of **1**, the yielded crude product **9** (2.34 g) was subjected to the following synthesis without further purification and characterization.

*2.1.10. 1-(2-Hydroxy-5-methylphenyl)-3-(thiophen-2-yl)propane-1,3-dione (**10**)*

1.5 g 1-(2-Hydroxy-5-methylphenyl)ethanone (10 mmol) and 2.19 g thiophene-2-carbonylchloride (15 mmol) were treated by the procedure used for the synthesis of **1**, giving 1.95 g **10** as yellow powder, yield 75%; ^{1}H NMR (400 MHz, $CDCl_3$) δ 15.74 (s, 1H), 11.75 (s, 1H), 7.80 (dd, J = 3.8, 1.1 Hz, 1H), 7.61 (dd, J = 5.0, 1.0 Hz, 1H), 7.49 (d, J = 1.3 Hz, 1H), 7.26–7.29 (m, 1H), 7.18 (dd, J = 4.9, 3.9 Hz, 1H), 6.90 (d, J = 8.5 Hz, 1H), 6.68 (s, 1H), 2.34 (s, 3H).

*2.1.11. 1-(2-Hydroxy-4-methoxyphenyl)-3-(thiophen-2-yl)propane-1,3-dione (**11**)*

1.66 g 1-(2-Hydroxy-4-methoxyphenyl)ethanone (10 mmol) and 2.19 g thiophene-2-carbonylchloride (15 mmol) were treated by the procedure used for the synthesis of **1**, giving 2.5 g **11** as yellow powder, yield 91%; ^{1}H NMR (400 MHz, $CDCl_3$) δ 15.45 (s, 1H), 12.47 (s, 1H), 7.75 (dd, J = 3.8, 1.1 Hz, 1H), 7.64 (d, J = 8.9 Hz, 1H), 7.57 (dd, J = 5.0, 1.1 Hz, 1H), 7.16 (dd, J = 5.0, 3.8 Hz, 1H), 6.57 (s, 1H), 6.48 (dd, J = 8.9, 2.5 Hz, 1H), 6.45 (d, J = 2.5 Hz, 1H), 3.85 (s, 3H).

*2.1.12. 1-(4-Bromophenyl)-3-(2-hydroxyphenyl)propane-1,3-dione (**12**)*

1.36 g 2-Hydroxyacetophenone (10 mmol) and 3.28 g 4-bromobenzoyl chloride (15 mmol) were treated by the procedure used for the synthesis of **1**, giving 2.39 g **12** as yellow crystal, yield 75%; ^{1}H NMR (400 MHz, $CDCl_3$) δ 15.49 (1H), 12.00 (1H), 7.78 (dd, J = 13.9, 7.6 Hz, 3H), 7.63 (d, J = 8.0 Hz, 2H), 7.47 (t, J = 7.8 Hz, 1H), 7.01 (d, J = 8.4 Hz, 1H), 6.93 (t, J = 7.6 Hz, 1H), 6.81 (1H).

*2.1.13. 1-(2-Hydroxyphenyl)-3-(thiophen-2-yl)propane-1,3-dione (**13**)*

1.36 g 2-Hydroxyacetophenone (10 mmol) and 2.19 g thiophene-2-carbonylchloride (15 mmol) were treated by the procedure used for the synthesis of **1**, giving 1.62 g **13** as yellow powder, yield 66%; ^{1}H NMR (400 MHz, $CDCl_3$) δ 15.65(1H), 11.96 (1H), 7.79 (d, J = 3.8 Hz, 1H), 7.73 (d, J = 8.1 Hz, 1H), 7.61 (d, J = 4.9 Hz, 1H), 7.46 (t, J = 7.8 Hz, 1H), 7.17 (t, J = 4.3 Hz, 1H), 6.99 (d, J = 8.4 Hz, 1H), 6.92 (t, J = 7.6 Hz, 1H), 6.69 (s,1H).

*2.1.14. 1-(2-Hydroxyphenyl)-3-(4-methoxyphenyl)propane-1,3-dione (**14**)*

1.36 g 2-Hydroxyacetophenone (10 mmol) and 2.56 g 4-methoxybenzoyl chloride (15 mmol) were treated by the procedure used for the synthesis of **1**, giving 1.67 g **14** as yellow crystal, yield 62%; ^{1}H NMR (400 MHz, $CDCl_3$) δ 15.76 (1H), 12.13 (1H),7.95 (dd, J = 31.0, 7.8 Hz, 2H), 7.76 (d, J = 7.9 Hz, 1H), 7.44 (t, J = 7.6 Hz, 1H), 6.98 (d, J = 7.2 Hz, 3H), 6.91 (t, J = 7.4 Hz, 1H), 6.76 (s,1H), 3.88 (3H).

*2.1.15. 1-(2-Hydroxyphenyl)-3-(naphthalen-2-yl)propane-1,3-dione (**15**)*

1.36 g 2-Hydroxyacetophenone (10 mmol) and 2.85 g 2-naphthoyl chloride (15 mmol) were treated by the procedure used for the synthesis of **1,** giving 2.4 g **15** as brown powder, yield 83%; ^{1}H NMR (400 MHz, $CDCl_3$) δ 15.62 (1H), 12.11 (1H), 8.49 (s, 1H),7.96–7.93 (m, 1H), 7.91 (s,2H), 7.87 (d, J = 7.6 Hz, 1H), 7.82 (d, J = 7.5 Hz, 1H), 7.60–7.52 (m, 2H), 7.46 (t, J = 7.3 Hz, 1H), 7.01 (d, J = 8.3 Hz, 1H), 6.96–6.91 (m, 2H).

2.1.16. tert-*Butyl 2-(1-(furan-2-yl)-7-methyl-9-oxo-2,9-dihydrochromeno[2,3-c]pyrrol-3-yl)acetate (**16**)*

244 mg **3** (1 mmol), 741 mg Fmoc-Asp(O^{t}Bu)-OH (1.8 mmol) and 49 mg DMAP (0.4 mmol) were dissolved in pyridine (10 mL), and then 412 mg DCC (2 mmol) was added. The mixture was stirred at room temperature about 3 h until **3** disappeared as monitored by TLC. The reaction temperature was raised to 50 °C for 4–6 h, and a major yellow spot could be observed by TLC. After the reaction mixture was evaporated under vacuum, 15 mL EtOAc was added and side product DCU was filtered. The filtrate was evaporated and subjected to column chromatography to afford 133 mg **16** as yellow powder, yield 35%; ^{1}H NMR (400 MHz, $CDCl_3$) δ 9.76 (s, 1H), 8.10 (s, 1H), 7.87 (d, J = 3.4 Hz, 1H), 7.45 (s, 1H), 7.39 (dd, J = 8.5, 2.1 Hz, 1H), 7.23 (d, J = 8.5 Hz, 1H), 6.55 (dd, J = 3.4, 1.8 Hz, 1H), 3.82 (2H), 2.43 (3H), 1.53 (9H); ^{13}C NMR (101 MHz, DMSO) δ 173.47, 168.77, 154.26, 146.03, 142.56, 142.07, 134.94, 132.03, 125.67, 121.63, 118.33, 117.18, 112.21, 109.35, 106.98, 106.38, 80.57, 30.36, 27.71 × 3, 20.23; HRMS calcd. for $C_{22}H_{21}NO_5[M+H]^+$: 380.1492, found, 380.1509.

2.1.17. tert-*Butyl 3-(1-(furan-2-yl)-7-methoxy-9-oxo-2,9-dihydrochromeno[2,3-c]pyrrol-3-yl)propanote (**17**)*

260 mg **8** (1 mmol), 766 mg Fmoc-Glu(O^{t}Bu)-OH (1.8 mmol), 49 mg DMAP (0.4 mmol) and 412 mg DCC (2 mmol) were treated with the procedure used for the synthesis of **16** to afford 225 mg **17** as yellow powder, yield 55%, ^{1}H NMR (400 MHz, $CDCl_3$) δ 9.86 (1H), 7.86 (d, J = 3.4 Hz, 1H), 7.75 (d, J = 3.1 Hz, 1H), 7.46–7.44 (m, 1H), 7.29 (d, J = 9.2 Hz, 1H), 7.20 (dd, J = 9.0, 2.9 Hz, 1H), 6.55 (dd, J = 2.9, 1.8 Hz, 1H), 3.91 (3H), 3.10 (2H), 2.68 (2H), 1.50 (9H); ^{13}C NMR (101 MHz, DMSO) δ 173.28, 171.21, 154.64, 150.66, 146.19, 142.37, 141.24, 122.34, 122.26, 118.75, 117.80, 112.18, 112.08, 108.99, 106.89, 106.10, 79.61, 55.46, 34.31, 27.57 × 3, 19.47; HRMS calcd for $C_{23}H_{23}NO_6[M+H]^+$: 410.1598, found, 410.1610.

2.1.18. tert-*Butyl 3-(1-(furan-2-yl)-7-methyl-9-oxo-2,9-dihydrochromeno[2,3-c]pyrrol-3-yl)propanoate (**18**)*

244 mg **3** (1 mmol), 766 mg Fmoc-Glu(O^{t}Bu)-OH (1.8 mmol), 49 mg DMAP (0.4 mmol) and 412 mg DCC (2 mmol) were treated with the procedure used for **16** to afford 118 mg **18** as yellow powder, yield 30%; ^{1}H NMR (400 MHz, $CDCl_3$) δ 9.82 (1H), 8.11 (s, 1H), 7.86 (d, J = 3.4 Hz, 1H), 7.45 (d, J = 1.0 Hz, 1H), 7.40 (dd, J = 8.5, 2.1 Hz, 1H), 7.25 (d, J = 8.5 Hz, 1H), 6.56 (dd, J = 3.4, 1.8 Hz, 1H), 3.10 (2H), 2.68 (2H), 1.50 (9H); ^{13}C NMR (101 MHz, DMSO) δ 173.54, 171.20, 154.32, 146.16, 142.39, 141.12, 134.86, 131.84, 125.64, 121.60, 118.02, 117.22, 112.18, 109.10, 106.41, 79.60, 34.31, 27.56 × 3, 20.23, 19.47; HRMS calcd. for $C_{23}H_{23}NO_5[M+H]^+$:394.1649, found, 394.1644.

*2.1.19. 3-(4-(*tert-*Butoxy)benzyl)-1-(furan-2-yl)-7-methylchromeno[2,3-c]pyrrol-9(2H)-one (**19**)*

244 mg **3** (1 mmol), 827 mg Fmoc-Tyr(^{t}Bu)-OH (1.8 mmol), 49 mg DMAP (0.4 mmol) and 412 mg DCC (2 mmol) were treated with the procedure used for **16** to afford 106 mg **19** as yellow powder, yield 25%; ^{1}H NMR (400 MHz, DMSO) δ 12.57 (1H), 7.95 (s,1H), 7.84 (s,1H), 7.74 (d, J = 3.4 Hz, 1H), 7.54–7.49 (m, 1H), 7.36 (d, J = 8.5 Hz, 1H), 7.19 (d, J = 8.3 Hz, 2H), 6.90 (d, J = 8.3 Hz, 2H), 6.68–6.65 (m, 1H), 4.10 (2H), 2.40 (3H), 1.25 (9H); ^{13}C NMR (101 MHz, DMSO) δ 173.59, 154.38, 153.28, 146.13, 142.45, 141.22, 134.92, 134.14, 131.98, 128.55 × 2, 125.65, 123.67 × 2, 121.67, 118.01, 117.32, 112.79, 112.22, 109.20, 106.58, 77.62, 28.47 × 3, 20.25; HRMS calcd. for $C_{27}H_{25}NO_4[M+H]^+$: 428.1856, found, 428.1863.

*2.1.20. 3-(4-(*tert-*Butoxy)benzyl)-1-(furan-2-yl)chromeno[2,3-c]pyrrol-9(2H)-one (**20**)*

230 mg **2** (1 mmol), 828 mg Fmoc-Tyr(^{t}Bu)-OH (1.8 mmol), 49 mg DMAP (0.4 mmol) and 412 mg DCC (2 mmol) were treated

with the procedure used for **16** to afford 194 mg **20** as yellow powder, yield 47%; ^{1}H NMR (400 MHz, DMSO) δ 12.60 (1H), 8.19 (dd, J = 7.9, 1.6 Hz, 1H), 7.83–7.81 (m, 1H), 7.79–7.76 (m, 1H), 7.71 (dt, J = 6.5, 2.7 Hz, 1H), 7.47 (d, J = 8.4 Hz, 1H), 7.37–7.31 (m, 1H), 7.21 (d, J = 8.5 Hz, 2H), 6.91 (d, J = 8.5 Hz, 2H), 6.69 (dd, J = 3.4, 1.8 Hz, 1H), 4.12 (2H), 1.25 (9H); ^{13}C NMR (101 MHz, DMSO) δ 173.51, 156.18, 153.28, 146.09, 142.51, 141.13, 134.12, 133.98, 128.56 × 2, 126.21, 123.69 × 2, 122.87, 122.04, 118.18, 117.51, 112.95, 112.24, 109.31, 106.50, 77.60, 28.45 × 3; HRMS calcd. for $C_{26}H_{23}NO_4$[M+H]$^+$: 414.1700, found, 414.1719.

2.1.21. tert-*Butyl 3-(1-(furan-2-yl)-9-oxo-2,9-dihydrochromeno[2,3-c]pyrrol-3-yl)propanoate (**21**)*

230 mg **2** (1 mmol), 766 mg Fmoc-Glu(O^{t}Bu)-OH (1.8 mmol), 49 mg DMAP (0.4 mmol) and 412 mg DCC (2 mmol) were treated with the procedure used for **16** to afford 170 mg **21** as brown powder, yield 45%; ^{1}H NMR (400 MHz, DMSO) δ 12.36 (1H), 8.15 (dd, J = 7.9, 1.5 Hz, 1H), 7.80 (s, 1H), 7.74–7.67 (m, 2H), 7.46 (d, J = 8.2 Hz, 1H), 7.32 (t, J = 7.5 Hz, 1H), 6.66 (dd, J = 3.3, 1.8 Hz, 1H), 3.02 (2H), 2.68 (2H), 1.31 (9H); ^{13}C NMR (101 MHz, DMSO) δ 173.96, 171.69, 156.61, 146.56, 143.00, 141.50, 134.49, 126.68, 123.30, 122.44, 118.67, 117.96, 112.88, 112.71, 109.71, 106.80, 80.16, 34.79, 28.07 × 3, 19.97; HRMS calcd. for $C_{22}H_{21}NO_5$[M+H]$^+$: 380.1492, found, 380.1506.

2.1.22. tert-*Butyl 3-(7-bromo-1-(furan-2-yl)-9-oxo-2,9-dihydrochromeno[2,3-c]pyrrol-3-yl)propanoate (**22**)*

309 mg **4** (1 mmol), 766 mg Fmoc-Glu(O^{t}Bu)-OH (1.8 mmol), 49 mg DMAP (0.4 mmol) and 412 mg DCC (2 mmol) were treated with the procedure used for **16** to afford 342 mg **22** as yellow powder, yield 75%; ^{1}H NMR (400 MHz, DMSO) δ 12.19 (1H), 8.18 (d, J = 2.5 Hz, 1H), 7.83 (dd, J = 7.6, 3.7 Hz, 2H), 7.71 (d, J = 3.1 Hz, 1H), 7.44 (d, J = 8.9 Hz, 1H), 6.68 (dd, J = 3.3, 1.7 Hz, 1H), 3.00 (2H), 2.89 (2H), 1.33 (9H); ^{13}C NMR (101 MHz, DMSO) δ 171.99, 171.16, 155.08, 145.85, 142.67, 140.80, 136.36, 128.24, 123.57, 120.06, 118.55, 114.72, 112.66, 112.23, 109.48, 105.80, 79.65, 34.19, 27.57 × 3, 19.41; HRMS calcd. for $C_{22}H_{20}NO_5Br$[M+H]$^+$: 458.0598, found, 458.0592.

*2.1.23. 1-(4-Bromophenyl)-3-(4-(*tert-*butoxy)benzyl)chromeno[2,3-c]pyrrol-9(2H)-one (**23**)*

319 mg **12** (1 mmol), 828 mg Fmoc-Tyr(^{t}Bu)-OH (1.8 mmol), 49 mg DMAP (0.4 mmol) and 412 mg DCC (2 mmol) were treated with the procedure used for **16** to afford 280 mg **23** as yellow powder, yield 56%; ^{1}H NMR (400 MHz, DMSO) δ 12.47(1H), 8.13 (dd, J = 32.4, 7.9 Hz, 3H), 7.69 (dd, J = 18.7, 7.7 Hz, 3H), 7.49 (d, J = 8.5 Hz, 1H), 7.34 (t, J = 7.1 Hz, 1H), 7.21 (d, J = 8.2 Hz, 2H), 6.91 (d, J = 8.2 Hz, 2H), 4.14 (2H), 1.25 (9H); ^{13}C NMR (101 MHz, DMSO) δ 174.10, 155.91, 153.36, 141.91, 133.99, 133.89, 131.02 × 2, 130.06, 129.49 × 2, 128.54 × 2, 126.40, 126.03, 123.72 × 2, 122.79, 121.90, 120.72, 117.40, 113.68, 107.65, 77.62, 28.52, 28.46 × 3; HRMS calcd. for $C_{28}H_{24}NO_3Br$[M+H]$^+$: 502.1012, found, 502.0999.

2.1.24. tert-*Butyl 3-(7-methoxy-9-oxo-1-(thiophen-2-yl)-2,9-dihydrochromeno[2,3-c]pyrrol-3-yl)propnoate (**24**)*

276 mg **9** (1 mmol), 766 mg Fmoc-Glu(O^{t}Bu)-OH (1.8 mmol), 49 mg DMAP (0.4 mmol) and 412 mg DCC (2 mmol) were treated with the procedure used for **16** to afford 297 mg **24** as yellow powder, yield 70%; ^{1}H NMR (400 MHz, DMSO) δ 12.15 (1H), 8.00 (d, J = 3.6 Hz, 1H), 7.57 (dd, J = 8.6, 4.0 Hz, 2H), 7.44 (d, J = 9.1 Hz, 1H), 7.32 (dd, J = 9.1, 3.1 Hz, 1H), 7.17–7.13 (m, 1H), 3.02 (2H), 2.69 (2H), 1.33 (9H); ^{13}C NMR (101 MHz, DMSO) δ 173.57, 171.18, 154.64, 150.58, 141.23, 133.25, 127.25, 126.05, 125.94, 122.41, 122.17, 121.37, 118.71, 112.07, 107.02, 106.59, 79.71, 55.50, 34.36, 27.61 × 3, 19.54; HRMS calcd. for $C_{23}H_{23}NO_5S$[M+H]$^+$: 426.1370, found, 426.1378.

*2.1.25. 3-(4-(*tert-*Butoxy)benzyl)-7-methoxy-1-(thiophen-2-yl)chromeno[2,3-c]pyrrol-9(2H)-one (**25**)*

276 mg **9** (1 mmol), 829 mg Fmoc-Tyr(^{t}Bu)-OH(1.8 mmol), 49 mg DMAP (0.4 mmol) and 412 mg DCC (2 mmol) were treated with the procedure used for **16** to afford 353 mg **25** as yellow powder, yield 77%; ^{1}H NMR (400 MHz, DMSO) δ 12.35 (1H), 8.02 (d, J = 3.5 Hz, 1H), 7.57 (dd, J = 13.4, 3.9 Hz, 2H), 7.43 (d, J = 9.1 Hz, 1H), 7.31 (dd, J = 9.0, 3.0 Hz, 1H), 7.20–7.13 (m, 3H), 6.91 (d, J = 8.4 Hz, 2H), 4.11 (1H), 3.85 (3H), 1.25 (9H); ^{13}C NMR (101 MHz, $CDCl_3$) δ 175.34, 155.11, 154.23, 151.58, 142.37, 133.19, 132.81, 128.88 × 2, 127.84, 126.35, 125.23, 124.52 × 2, 123.28, 122.69, 122.56, 118.63, 111.71, 107.98, 106.77, 78.51, 55.77, 29.32, 28.82 × 3; HRMS calcd. for $C_{27}H_{25}NO_4S$[M+H]$^+$: 460.1577, found, 460.1564.

2.1.26. tert-*Butyl 3-(9-oxo-1-phenyl-2,9-dihydrochromeno[2,3-c]pyrrol-3-yl)propanoate (**26**)*

240 mg **1** (1 mmol), 766 mg Fmoc-Glu(O^{t}Bu)-OH (1.8 mmol), 49 mg DMAP (0.4 mmol) and 412 mg DCC (2 mmol) were treated with the procedure used for **16** to afford 318 mg **26** as yellow powder, yield 82%; ^{1}H NMR (400 MHz, DMSO) δ 12.16 (1H), 8.11 (dd, J = 29.6, 7.1 Hz, 3H), 7.68 (d, J = 6.7 Hz, 1H), 7.46 (s, 3H), 7.33 (dd, J = 14.5, 7.0 Hz, 2H), 3.04 (2H), 2.70 (2H), 1.32 (9H); ^{13}C NMR (101 MHz, DMSO) δ 174.01, 171.23, 155.91, 141.56, 133.84, 130.96, 128.08 × 2, 127.66 × 2, 127.56, 127.37, 126.37, 122.61, 121.92, 117.32, 112.58, 107.14, 79.67, 34.34, 27.58 × 3, 19.56; HRMS calcd. for $C_{24}H_{23}NO_4$[M+H]$^+$: 390.1700, found, 390.1697.

27–**32** were used as intermediates and not characterized.

*2.1.27. 3-(4-(*tert-*Butoxy)benzyl)-1-(4-fluorophenyl)-7-methylchromeno[2,3-c]pyrrol-9(2H)-one (**27**)*

272 mg **7** (1 mmol), 828 mg Fmoc-Tyr(^{t}Bu)-OH (1.8 mmol), 49 mg DMAP (0.4 mmol) and 412 mg DCC (2 mmol) were treated with the procedure used for **16** to afford 254 mg **27**.

2.1.28. tert-*Butyl3-(7-bromo-9-oxo-1-(thiophen-2-yl)-2,9-dihydrochromeno[2,3-c]pyrrol-3-yl) propanoate (**28**)*

325 mg **5** (1 mmol) and 766 mg Fmoc-Glu(O^{t}Bu)-OH (1.8 mmol), 48.8 mg DMAP (0.4 mmol) and 412 mg DCC (2 mmol) were treated with the procedure used for **16** to afford 142 mg **28**.

*2.1.29. 7-Bromo-3-(4-(*tert-*butoxy)benzyl)-1-(thiophen-2-yl)chromeno[2,3-c]pyrrol-9(2H)-one (**29**)*

325 mg **5** (1 mmol), 828 mg Fmoc-Tyr(^{t}Bu)-OH (1.8 mmol), 49 mg DMAP (0.4 mmol) and 412 mg DCC (2 mmol) were treated with the procedure used for **16** to afford 142 mg **29**.

2.1.30. tert-*Butyl 3-(1-(4-fluorophenyl)-7-methyl-9-oxo-2,9-dihydrochromeno[2,3-c]pyrrol-3-yl) propanoate (**30**)*

272 mg **7** (1 mmol), 766 mg Fmoc-Glu(O^{t}Bu)-OH (1.8 mmol), 49 mg DMAP (0.4 mmol) and 412 mg DCC (2 mmol) were treated with the procedure used for **16** to afford 193 mg **30**.

*2.1.31. 3-(4-(*tert-*Butoxy)benzyl)-1-(thiophen-2-yl)chromeno[2,3-c]pyrrol-9(2H)-one (**31**)*

246 mg **13** (1 mmol), 828 mg Fmoc-Tyr(^{t}Bu)-OH(1.8 mmol), 49 mg DMAP (0.4 mmol) and 412 mg DCC (2 mmol) were treated with the procedure used for **16** to afford 280 mg **31**.

*2.1.32. 3-(4-(*tert-*Butoxy)benzyl)-1-(4-methoxyphenyl)chromeno[2,3-c]pyrrol-9(2H)-one (**32**)*

270 mg **14** (1 mmol), 828 mgFmoc-Tyr(^{t}Bu)-OH (1.8 mmol), 49 mg DMAP (0.4 mmol) and 412 mg DCC (2 mmol) were treated with the procedure used for **16** to afford 100 mg **32**.

*2.1.33. 3-benzyl-1-(naphthalen-2-yl)chromeno[2,3-c]pyrrol-9(2H)-one (**33**)*

290 mg **15** (1 mmol), 697 mg Fmoc-Phe-OH (1.8 mmol), 49 mg DMAP (0.4 mmol) and 412 mg DCC (2 mmol) were treated with the procedure used for **16** to afford 148 mg **33** as yellow powder, yield 37%; ^{1}H NMR (400 MHz, DMSO) δ 12.56 (1H), 8.66 (s, 1H), 8.25–8.19 (m, 2H), 8.02–7.92 (m, 3H), 7.73 (ddd, J = 8.6, 7.1, 1.7 Hz, 1H), 7.57–7.49 (m, 3H), 7.38–7.32 (m, 5H), 7.21 (dd, J = 9.4, 4.3 Hz, 1H), 4.23 (2H); ^{13}C NMR (101 MHz, DMSO) δ 174.10, 155.98, 141.96, 139.48, 133.95, 132.76, 132.24, 128.49 × 2, 128.10 × 2, 128.08, 127.51, 127.42, 127.38, 126.46, 126.43, 126.29, 126.22, 126.17, 125.96, 122.79, 122.03, 117.42, 113.40, 107.71, 29.35; HRMS calcd. for $C_{28}H_{19}NO_2$ $[M+H]^+$: 402.1489, found, 402.1506.

*2.1.34. 3-(4-(*tert*-Butoxy)benzyl)-1-(naphthalen-2-yl)chromeno[2,3-c]pyrrol-9(2H)-one (**34**)*

290 mg **15** (1 mmol), 828 mg Fmoc-Tyr(^{t}Bu)-OH (1.8 mmol), 49 mg DMAP (0.4 mmol) and 412 mg DCC (2 mmol) were treated with the procedure used for **16** to afford 203 mg **34** as yellow powder, yield 43%; ^{1}H NMR (400 MHz, DMSO) δ 12.55 (1H), 8.69 (1H), 8.28–8.20 (m, 2H), 8.03–7.92 (m, 3H), 7.71 (d, J = 7.0 Hz, 1H), 7.58–7.47 (m, 3H), 7.40–7.33 (m, 1H), 7.25 (d, J = 7.6 Hz, 2H), 6.93 (d, J = 7.7 Hz, 2H), 4.19 (2H), 1.25 (9H); ^{13}C NMR (101 MHz, DMSO) δ 174.10, 155.98, 153.36, 141.94, 134.04, 133.95, 132.76, 132.23, 128.58 × 2, 128.48, 128.07, 127.51, 127.38, 126.47, 126.43, 126.27, 126.22, 125.94, 123.74 × 2, 122.78, 122.04, 117.41, 113.55, 107.70, 77.63, 28.60, 28.47 × 3; HRMS calcd. for $C_{32}H_2NO_3$[M+H]$^+$: 474.2064, found, 474.2051.

2.1.35. tert*-Butyl 2-(7-methoxy-9-oxo-1-(thiophen-2-yl)-2,9-dihydrochromeno[2,3-c]pyrrol-3-yl)acetate (**35**)*

276 mg **9** (1 mmol), 741 mg Fmoc-Asp(O^{t}Bu)-OH (1.8 mmol), 49 mg DMAP (0.4 mmol) and 412 mg DCC (2 mmol) were treated with the procedure used for **16** to afford 279 mg **35** as yellow powder, yield 68%; ^{1}H NMR (400 MHz, DMSO) δ 12.31 (1H), 8.03 (d, J = 2.8 Hz, 1H), 7.61–7.56 (m, 2H), 7.43 (d, J = 9.1 Hz, 1H), 7.32 (dd, J = 9.0, 3.1 Hz, 1H), 7.18–7.14 (m, 1H), 3.85 (3H), 3.77 (2H), 1.44 (9H); ^{13}C NMR (101 MHz, DMSO) δ 173.49, 168.77, 154.72, 150.46, 142.18, 133.10, 127.38, 126.26, 126.16, 122.52, 122.19, 121.82, 118.69, 106.98, 106.82, 106.52, 80.72, 55.50, 30.42, 27.72 × 3; HRMS calcd. for $C_{22}H_{21}NO_5S$[M+H]$^+$: 412.1213, found, 412.1228.

*2.1.36. 3-Benzyl-1-(4-bromophenyl)chromeno[2,3-c]pyrrol-9(2H)-one (**36**)*

319 mg **12** (1 mmol), 697 mg Fmoc-Phe-OH (1.8 mmol), 49 mg DMAP (0.4 mmol) and 412 mg DCC (2 mmol) were treated with the procedure used for **16** to afford 270 mg **36** as yellow powder, yield 63%; ^{1}H NMR (400 MHz, DMSO) δ 12.48 (1H), 8.17 (dd, J = 7.9, 1.5 Hz, 1H), 8.09 (d, J = 8.6 Hz, 2H), 7.74–7.69 (m, 1H), 7.67 (d, J = 8.6 Hz, 2H), 7.48 (d, J = 8.3 Hz, 1H), 7.35 (d, J = 7.9 Hz, 1H), 7.32 (d, J = 4.1 Hz, 4H), 7.21 (dd, J = 8.4, 4.6 Hz, 1H), 4.19 (2H); ^{13}C NMR (101 MHz, DMSO) δ 174.58, 156.40, 142.41, 139.81, 134.51, 131.52 × 2, 130.54, 130.00 × 2, 128.96 × 2, 128.54 × 2, 126.89, 126.67, 126.54, 123.30, 122.38, 121.24, 117.91, 114.03, 108.14, 29.78; HRMS calcd. for $C_{24}H_{16}NO_2Br$ $[M+H]^+$: 430.0437, found, 430.0431.

The synthesis of compounds **37**, **41**–**47** was previously reported [41].

2.1.37. tert*-Butyl 2-(1-(4-fluorophenyl)-9-oxo-2,9-dihydrochromeno[2,3-c]pyrrol-3-yl)acetate (**38**)*

258 mg **6** (1 mmol), 741 mg Fmoc-Asp(O^{t}Bu)-OH (1.8 mmol), 49 mg DMAP (0.4 mmol) and 412 mg DCC (2 mmol) were treated with the procedure used for **16** to afford 122 mg **38** as yellow powder, yield 31%; ^{1}H NMR (400 MHz, DMSO) δ 12.34 (1H), 8.14 (dd, J = 8.6, 5.8 Hz, 3H), 7.70 (t, J = 7.1 Hz, 1H), 7.45 (d, J = 8.3 Hz, 1H), 7.31 (dd, J = 12.1, 5.7 Hz, 3H), 3.78 (2H), 1.43 (9H); ^{13}C NMR (101 MHz, DMSO) δ 173.97, 168.78, 162.92, 160.48, 155.84, 142.42, 133.98, 129.82, 129.74, 127.37, 127.34, 126.82, 126.38, 122.79, 121.86, 117.28, 115.18, 114.97, 107.34, 107.05, 80.70, 30.45, 27.70 × 3; HRMS calcd. for $C_{23}H_{20}NO_4F$ $[M+H]^+$: 394.1449, found, 394.1464.

2.1.38. tert*-Butyl 2-(1-(4-fluorophenyl)-7-methyl-9-oxo-2,9-dihydrochromeno[2,3-c]pyrrol-3-yl)acetate (**39**)*

272 mg **7** (1 mmol), 741 mg Fmoc-Asp(O^{t}Bu)-OH (1.8 mmol), 49 mg DMAP (0.4 mmol) and 412 mg DCC (2 mmol) were treated with the procedure used for **16** to afford 260 mg **39** as yellow powder, yield 64%; ^{1}H NMR (400 MHz, DMSO) δ 12.31 (1H), 8.13 (dd, J = 8.4, 5.6 Hz, 2H), 7.93 (s, 1H), 7.51 (d, J = 8.4 Hz, 1H), 7.32 (dd, J = 16.3, 8.4 Hz, 3H), 3.77 (2H), 2.38 (3H), 1.43 (9H); ^{13}C NMR (101 MHz, DMSO) δ 174.04, 168.80, 162.88, 160.44, 154.06, 142.52, 134.94, 131.87, 129.79, 129.71, 127.44, 127.41, 126.64, 125.83, 121.50, 117.09, 115.17, 114.96, 107.17, 80.69, 30.46, 27.71 × 3, 20.28; HRMS calcd. for $C_{24}H_{22}NO_4F$ $[M+H]^+$: 408.1606, found, 408.1605.

2.1.39. tert*-Butyl 3-((1-(4-fluorophenyl)-9-oxo-2,9-dihydrochromeno[2,3-c]pyrrol-3-yl)methyl)-1H-indole-1-carboxylate (**40**)*

258 mg **6** (1 mmol), 948 mg Fmoc-Trp(BOC)-OH (1.8 mmol), 49 mg DMAP (0.4 mmol) and 412 mg DCC (2 mmol) were treated with the procedure used for **16** to afford 213 mg **40** as yellow powder, yield 42%; ^{1}H NMR (400 MHz, DMSO) δ 12.36 (1H), 8.16 (dd, J = 7.9, 1.5 Hz, 1H), 8.11 (dd, J = 8.8, 5.5 Hz, 2H), 8.03 (d, J = 8.1 Hz, 1H), 7.74 (t, J = 6.3 Hz, 2H), 7.56–7.50 (m, 2H), 7.36–7.28 (m, 4H), 7.24 (t, J = 7.2 Hz, 1H), 4.21 (2H), 1.61 (9H); ^{13}C NMR (101 MHz, DMSO) δ 174.05, 155.95, 149.03, 141.32, 134.78, 134.03, 129.99 × 2, 129.91 × 2, 129.68, 127.37, 126.67, 126.38, 124.44, 123.37, 122.80, 122.57, 121.88, 119.11, 118.24, 117.32, 115.09, 114.87, 114.73, 111.86, 107.14, 83.61, 27.63 × 3, 19.21; HRMS calcd. for $C_{31}H_{25}N_2O_4F$ $[M+H]^+$: 509.1871, found, 509.1859.

2.1.40. tert*-Butyl (4-(7-methoxy-9-oxo-1-(thiophen-2-yl)-2,9-dihydrochromeno[2,3-c]pyrrol-3-yl)butyl) carbamate (**48**)*

276 mg **9** (1 mmol), 843 mg Fmoc-Lys(BOC)-OH (1.8 mmol), 49 mg DMAP (0.4 mmol) and 412 mg DCC (2 mmol) were treated with the procedure used for **16** to afford 351 mg **48** as brown powder, yield 75%; ^{1}H NMR (400 MHz, DMSO) δ 12.14 (1H), 8.00 (s, 1H), 7.59 (s, 1H), 7.55 (d, J = 3.4 Hz, 1H), 7.44 (d, J = 8.9 Hz, 1H), 7.31 (d, J = 9.0 Hz, 1H), 7.16 (s, 1H), 6.78 (1H), 3.85 (3H), 2.98 (2H), 2.79 (2H), 1.68 (2H), 1.47 (2H), 1.36 (9H); ^{13}C NMR (101 MHz, DMSO) δ 173.65, 155.55, 154.59, 150.66, 141.04, 133.35, 127.21, 125.89, 125.79, 122.37, 122.18, 120.90, 118.75, 113.86, 106.94, 106.64, 77.28, 55.49, 29.13, 28.20 × 3, 26.39, 23.15; HRMS calcd. for $C_{25}H_{28}N_2O_5S$ $[M+H]^+$: 469.1792, found, 469.1793.

*2.1.41. 1-([1,1′-biphenyl]-4-yl)-3-(4-(*tert*-butoxy)benzyl)chromeno[2,3-c]pyrrol-9(2H)-one (**49**)*

250 mg **23** (0.5 mmol), 79 mg phenyl boronic acid (0.65 mmol) and 25 mg dichloro(1,10-bis(diphenylphosphino)ferrocene) palladium(II)-dichloromethane adduct ($PdCl_2$ (dppf), 0.03 mmol) were dissolved in 2 ml dioxane, and 2 ml 2 M K_2CO_3 was added. React in microwave at 150 °C for 20 min, monitored by using TLC. Then 20 ml ethyl acetate was added and washed with water, organic layer was evaporated and subjected to column chromatography to afford 205 mg **49** as yellow powder, yield 82%; ^{1}H NMR (400 MHz, DMSO) δ 12.45 (1H), 8.22 (dd, J = 19.5, 8.0 Hz, 3H), 7.82–7.69 (m, 5H), 7.50 (t, J = 7.7 Hz, 3H), 7.43–7.32 (m, 2H), 7.23 (d, J = 8.2 Hz, 2H), 6.92 (d, J = 8.2 Hz, 2H), 4.16 (2H), 1.25 (9H); ^{13}C NMR (101 MHz, DMSO) δ 174.06, 155.93, 153.35, 141.89, 139.52, 139.04, 134.05, 133.91, 130.00, 128.91 × 2, 128.56 × 2, 128.09 × 2, 127.50,

127.09, 126.48 × 2, 126.27 × 2, 123.73 × 2, 122.74, 122.04, 117.38, 113.35, 107.56, 77.62, 28.56, 28.47 × 3; HRMS calcd. for $C_{34}H_2NO_3$ $[M-H]^-$: 498.2075, found, 498.2068.

*2.1.42. 3-(7-methoxy-9-oxo-1-(thiophen-2-yl)-2,9-dihydrochromeno[2,3-c]pyrrol-3-yl)propanoic acid (**50**)*

212 mg **24** (0.5 mmol) was dissolved in 20 ml CH_2Cl_2 and 5 ml TFA was dropped in. The mixture was stirred at room temperature until reactant disappeared as monitored by using TLC. Then the reaction mixture was evaporated in vacuum and subjected to column chromatography to yield 107 mg **50** as red powder, yield 58%; ^{1}H NMR (400 MHz, DMSO) δ 12.23 (1H), 12.16 (1H), 8.00 (s, 1H), 7.58 (s, 2H), 7.44 (d, J = 8.3 Hz, 1H), 7.32 (d, J = 7.5 Hz, 1H), 7.15 (s, 1H), 3.85 (3H), 3.04 (2H), 2.72 (2H); ^{13}C NMR (101 MHz, DMSO) δ 173.59, 173.49, 154.63, 150.62, 141.15, 133.25, 127.24, 126.02, 125.94, 122.39, 122.17, 121.23, 118.76, 112.37, 106.97, 106.67, 55.50, 33.11, 19.39; HRMS calcd. for $C_{19}H_{15}NO_5S$ $[M+H]^+$: 370.0744, found, 370.0759.

*2.1.43. 3-(4-hydroxybenzyl)-7-methoxy-1-(thiophen-2-yl)chromeno[2,3-c]pyrrol-9(2H)-one (**51**)*

The *tert*-butyl protection of **25** (229 mg, 0.5 mmol) was removed by dissolving **25** in 20 ml CH_2Cl_2 and 5 ml TFA with stir at room temperature until the reactant disappeared as monitored by TLC. The reaction mixture was evaporated in vacuum and subjected to column chromatography to afford 91 mg **51** as yellow powder, yield 45%; ^{1}H NMR (400 MHz, MeOD) δ 7.92 (d, J = 3.7 Hz, 1H), 7.66 (d, J = 3.0 Hz, 1H), 7.41 (d, J = 5.1 Hz, 1H), 7.35 (d, J = 9.1 Hz, 1H), 7.26 (dd, J = 9.1, 3.1 Hz, 1H), 7.10 (d, J = 8.6 Hz, 3H), 6.72 (d, J = 8.4 Hz, 2H), 4.09 (2H), 3.88 (3H); ^{13}C NMR (101 MHz, DMSO) δ 173.61, 155.69, 154.67, 150.62, 141.25, 133.26, 129.52, 128.92 × 2, 127.26, 126.05, 125.97, 122.43, 122.23, 121.26, 118.79, 115.19 × 2, 113.11, 106.98, 106.73, 55.51, 28.32; HRMS calcd. for $C_{23}H_{17}NO_4S$ $[M+H]^+$: 404.0951, found, 404.0951.

*2.1.44. 3-(9-Oxo-1-phenyl-2,9-dihydrochromeno[2,3-c]pyrrol-3-yl)propanoic acid (**52**)*

195 mg **26** (0.5 mmol) was treated with the procedure used for **50** to afford 117 mg **52** as yellow powder, yield 70%; ^{1}H NMR (400 MHz, DMSO) δ 12.18 (1H), 8.12 (dd, J = 30.4, 7.9 Hz, 3H), 7.72 (t, J = 7.6 Hz, 1H), 7.48 (dd, J = 14.7, 7.8 Hz, 3H), 7.38–7.30 (m, 2H), 3.07 (2H), 2.76 (2H); ^{13}C NMR (101 MHz, DMSO) δ 174.03, 173.55, 155.99, 141.46, 133.84, 130.95, 128.08 ×2, 127.70 × 2, 127.57, 127.24, 126.35, 122.63, 121.92, 117.39, 112.89, 107.21, 33.12, 19.41; HRMS calcd. for $C_{20}H_{15}NO_4$ $[M+H]^+$: 334.1074, found, 334.1081.

*2.1.45. 1-(4-Fluorophenyl)-3-(4-hydroxybenzyl)-7-methylchromeno[2,3-c]pyrrol-9(2H)-one (**53**)*

227 mg **27** (0.5 mmol) was treated with the procedure used for **50** to afford 112 mg **53** as yellow powder, yield 56%; ^{1}H NMR (400 MHz, DMSO) δ 12.30 (1H), 9.20 (1H), 8.13 (s, 2H), 7.94 (s, 1H), 7.51 (d, J = 8.2 Hz, 1H), 7.37 (d, J = 8.3 Hz, 1H), 7.30 (t, J = 8.3 Hz, 2H), 7.10 (d, J = 7.6 Hz, 2H), 6.70 (d, J = 7.7 Hz, 2H), 4.04 (2H), 2.40 (3H); ^{13}C NMR (101 MHz, DMSO) δ 174.17, 162.79, 160.34, 155.69, 154.21, 141.53, 134.87, 131.74, 129.86, 129.78, 129.58, 128.96 × 2, 127.56, 127.54, 126.09, 125.80, 121.54, 117.22, 115.18 × 2, 115.07, 114.86, 113.50, 107.28, 28.43, 20.29; HRMS calcd. for $C_{25}H_{18}NO_3F$ $[M+H]^+$: 400.1343, found, 400.1345.

*2.1.46. 3-(7-Bromo-9-oxo-1-(thiophen-2-yl)-2,9-dihydrochromeno[2,3-c]pyrrol-3-yl)propanoicacid (**54**)*

237 mg **28** (0.5 mmol) was treated with the procedure used for **50** to afford 135 mg **54** as yellow powder, yield 65%; ^{1}H NMR (400 MHz, DMSO) δ 12.26 (2H), 8.21–8.17 (m, 1H), 8.01 (m,1H), 7.86–7.81 (m, 1H), 7.58 (t, J = 4.5 Hz, 1H), 7.46 (dd, J = 8.8, 5.0 Hz, 1H), 7.16 (dd, J = 8.7, 5.0 Hz, 1H), 3.02 (2H), 2.72 (2H); ^{13}C NMR (101 MHz, DMSO) δ 173.47, 172.34, 155.02, 140.72, 136.40, 132.85, 128.30, 127.37, 126.44, 126.37, 123.50, 122.03, 120.11, 114.68, 112.97, 106.40, 33.03, 19.33; HRMS calcd. for $C_{18}H_{12}NO_4S$ Br$[M+H]^+$: 417.9743, found, 417.9741.

*2.1.47. 7-Bromo-3-(4-hydroxybenzyl)-1-(thiophen-2-yl)chromeno[2,3-c]pyrrol-9(2H)-one (**55**)*

254 mg **29** (0.5 mmol) was treated with the procedure used for **50** to afford 72 mg **55** as yellow powder, yield 32%; ^{1}H NMR (400 MHz, DMSO) δ 12.41 (1H), 9.21 (1H), 8.20 (d, J = 2.4 Hz, 1H), 8.02 (d, J = 3.2 Hz, 1H), 7.84 (dd, J = 8.8, 2.4 Hz, 1H), 7.58 (d, J = 4.9 Hz, 1H), 7.45 (d, J = 8.9 Hz, 1H), 7.19–7.14 (m, 1H), 7.08 (d, J = 8.3 Hz, 2H), 6.70 (d, J = 8.3 Hz, 2H), 4.04 (2H); ^{13}C NMR (101 MHz, DMSO) δ 172.39, 155.73, 155.06, 140.87, 136.41, 132.88, 129.29, 128.94 × 2, 128.35, 127.37, 126.43, 123.59, 122.08, 120.11, 115.20 × 2, 114.71, 113.69, 106.51, 28.28; HRMS calcd. for $C_{22}H_{14}NO_3SBr[M+H]^+$: 451.9951, found, 451.9961.

*2.1.48. 3-(1-(4-Fluorophenyl)-7-methyl-9-oxo-2,9-dihydrochromeno[2,3-c]pyrrol-3-yl)propanoic acid (**56**)*

210 mg **30** (0.5 mmol) was treated with the procedure used for **50** to afford 63.8 mg **56** as yellow powder, yield 35%; ^{1}H NMR (400 MHz, DMSO) δ 12.23 (2H), 8.15–8.09 (m, 2H), 7.93 (s, 1H), 7.53 (d, J = 8.3 Hz, 1H), 7.39 (d, J = 8.4 Hz, 1H), 7.31 (t, J = 8.8 Hz, 2H), 3.06 (2H), 2.74 (2H), 2.40 (3H); ^{13}C NMR (101 MHz, DMSO) δ 174.13, 173.55, 162.78, 160.34, 154.16, 141.45, 134.80, 131.64, 129.80, 129.72, 127.58, 127.55, 126.02, 125.75, 121.46, 117.17, 115.05, 114.84, 112.64, 107.19, 33.10, 20.27, 19.38; HRMS calcd. for $C_{21}H_{16}NO_4F[M+H]^+$: 366.1136, found, 366.1137.

*2.1.49. 3-(4-Hydroxybenzyl)-1-(thiophen-2-yl)chromeno[2,3-c]pyrrol-9(2H)-one (**57**)*

tert-Butyl protection of **31** (215 mg, 0.5 mmol) was removed with the procedure used for **51** to afford 112 mg of **57** as red crystal, yield 60%; ^{1}H NMR (400 MHz, DMSO) δ 12.33 (1H), 9.21 (1H), 8.16 (dd, J = 7.9, 1.4 Hz, 1H), 8.04–8.00 (m, 1H), 7.74–7.67 (m, 1H), 7.56 (d, J = 5.0 Hz, 1H), 7.47 (d, J = 8.2 Hz, 1H), 7.33 (t, J = 7.5 Hz, 1H), 7.15 (dd, J = 5.0, 3.8 Hz, 1H), 7.08 (d, J = 8.4 Hz, 2H), 6.69 (d, J = 8.5 Hz, 2H), 4.05 (2H); ^{13}C NMR (101 MHz, DMSO) δ 173.80, 156.06, 155.71, 141.03, 133.99, 133.16, 129.48, 128.93 × 2, 127.30, 126.27, 126.16, 122.79, 121.93, 121.65, 117.45, 115.20 × 2, 113.40, 106.98, 28.32; HRMS calcd. for $C_{22}H_{15}NO_3S$ $[M-H]^-$: 372.0700, found, 372.0703.

*2.1.50. 3-(4-Hydroxybenzyl)-1-(4-methoxyphenyl)chromeno[2,3-c]pyrrol-9(2H)-one (**58**)*

226 mg **32** (0.5 mmol) was treated with the procedure used for **50** to afford 111 mg **58** as brown crystal, yield 56%; ^{1}H NMR (400 MHz, DMSO) δ 12.16 (1H), 9.20 (1H), 8.10 (dd, J = 39.1, 6.3 Hz, 3H), 7.69 (t, 1H),7.46 (d, J = 6.9 Hz, 1H), 7.31 (t, 1H),7.06 (dd, J = 26.7, 6.2 Hz, 4H), 6.69 (d, J = 6.1 Hz, 2H), 4.04 (2H), 3.82 (3H); ^{13}C NMR (101 MHz, DMSO) δ 174.47, 159.42, 156.48, 156.16, 141.73, 134.29, 130.22, 129.66 × 2, 129.45 × 2, 128.22, 126.88, 124.07, 123.08, 122.51, 117.83, 115.67 × 2, 114.04 × 2, 113.26, 107.19, 55.67, 28.91; HRMS calcd. for $C_{25}H_{19}NO_4$ $[M-H]^-$: 396.1241, found, 396.1257.

*2.1.51. 3-(4-Hydroxybenzyl)-1-(naphthalen-2-yl)chromeno[2,3-c]pyrrol-9(2H)-one (**59**)*

237 mg **34** (0.5 mmol) was treated with the procedure used for **50** to afford 52 mg **59** as brown powder, yield 25%; ^{1}H NMR (400 MHz, DMSO) δ 12.51 (1H), 9.24 (1H), 8.67 (1H), 8.24 (ddd, J = 9.9, 8.3, 1.7 Hz, 2H), 8.01–7.92 (m, 3H), 7.72 (t, J = 8.6 Hz, 1H), 7.57–7.48 (m, 3H), 7.35 (dd, J = 11.1, 3.9 Hz, 1H), 7.16 (d, J = 8.5 Hz, 2H), 6.72 (dd, J = 6.6, 4.7 Hz, 2H), 4.12 (2H); ^{13}C NMR (101 MHz,

DMSO) δ 174.12, 156.00, 155.71, 141.72, 133.94, 132.76, 132.20, 129.59, 129.02 × 2, 128.52, 128.06, 127.50, 127.35, 127.18, 126.46, 126.42, 126.24, 126.20, 125.98, 122.75, 122.02, 117.43, 115.22 × 2, 114.22, 107.69, 28.50; HRMS calcd. for $C_{28}H_{19}NO_3$ $[M+H]^+$: 418.1438, found, 418.1446.

*2.1.52. 3-Benzyl-2-methyl-1-phenylchromeno[2,3-c]pyrrol-9(2H)-one (**60**)*

176 mg 3-Benzyl-1-phenylchromeno[2,3-*c*]pyrrol-9(2*H*)-one (**42**, 0.5 mmol) was dissolved in 20 ml CH_3CN or acetone, and 207 mg K_2CO_3 (1.5 mmol) was added. 355 mg CH_3I (2.5 mmol) was dropped into the mixture quickly, refluxed at 50 °C for 3 h until reactant disappeared, as monitored by using TLC. The reaction mixture was evaporated in vacuum, and then 20 ml EtOAc was added. The resulted solution was washed with 50 ml water and saturated salt solution. The organic layer was dried over anhydrous sodium sulfate, and the filtrate was evaporated and subjected to column chromatography to afford 142 mg **60** as light yellow powder, yield 78%; ^{1}H NMR (400 MHz, DMSO) δ 8.09 (d, *J* = 7.7 Hz, 1H), 7.70 (t, *J* = 7.6 Hz, 1H), 7.53 (t, *J* = 6.1 Hz,2H), 7.52–7.44 (m, 4H), 7.37–7.31 (m, 3H), 7.31–7.20 (m, 3H), 4.30 (2H), 3.48 (3H); ^{13}C NMR (101 MHz, DMSO) δ 173.03, 156.07, 141.47, 138.57, 133.80, 131.02 × 2, 129.70, 129.10, 128.68 × 2, 128.24, 127.99 × 2, 127.79 × 2, 126.34, 126.10, 122.74, 122.07, 117.54, 113.71, 107.23, 32.08, 28.18; HRMS calcd. for $C_{25}H_{19}NO_2$ $[M+H]^+$: 366.1489, found, 366.1503.

*2.1.53. 3-(4-Hydroxybenzyl)-1-phenylchromeno[2,3-c]pyrrol-9(2H)-one (**61**)*

The *tert*-butyl protection of **43** (212 mg, 0.5 mmol) was removed with the procedure used for **51** to afford 152 mg of **61** as yellow powder, yield 83%; ^{1}H NMR (400 MHz, DMSO) δ 12.39 (1H), 9.20 (1H), 8.17 (dd, *J* = 7.9, 1.6 Hz, 1H), 8.09 (d, *J* = 7.4 Hz, 2H), 7.71 (ddd, *J* = 8.6, 7.2, 1.7 Hz, 1H), 7.52–7.41 (m, 3H), 7.34 (dd, *J* = 14.6, 7.2 Hz, 2H), 7.11 (d, *J* = 8.4 Hz, 2H), 6.70 (d, *J* = 8.4 Hz, 2H), 4.06 (2H); ^{13}C NMR (101 MHz, DMSO) δ 174.05, 155.96, 155.69, 141.52, 133.88, 130.94, 129.61, 128.98 × 2, 128.07 × 2, 127.71 × 2, 127.57, 127.26, 126.40, 122.69, 121.98, 117.40, 115.19 × 2, 113.74, 107.30, 28.44; HRMS calcd. for $C_{24}H_{17}NO_3$ $[M+H]^+$: 368.1281, found, 368.1281.

*2.1.54. 3-(4-Hydroxybenzyl)-2-methyl-1-phenylchromeno[2,3-c]pyrrol-9(2H)-one (**62**)*

110 mg **61** (0.3 mmol) was dissolved in 10 ml acetone, and 124 mg K_2CO_3 (0.9 mmol) was added. 213 mg CH_3I (1.5 mmol) was dropped into the mixture quickly and refluxed at 50 °C for 3 h until reactant disappeared as monitored by using TLC. The reaction mixture was evaporated in vacuum, and 20 ml EtOAc was added. The resulted solution was washed with 50 ml water and saturated salt solution. The organic layer was dried over anhydrous sodium sulfate, and the filtrate was evaporated and subjected to column chromatography to afford 39 mg **62** as yellow powder, yield 34%; ^{1}H NMR (400 MHz, $CDCl_3$) δ 8.27 (d, *J* = 7.8 Hz, 1H), 7.60 (t, *J* = 7.6 Hz, 1H), 7.52 (d, *J* = 7.4 Hz, 2H), 7.47 (t, *J* = 7.1 Hz, 2H), 7.43 (d, *J* = 6.8 Hz, 1H), 7.38 (d, *J* = 8.3 Hz, 1H), 7.24 (d, *J* = 7.7 Hz, 1H), 7.10 (d, *J* = 7.9 Hz, 2H), 6.79 (d, *J* = 7.9 Hz, 2H), 5.02 (1H), 4.23 (2H), 3.46 (3H); ^{13}C NMR (101 MHz, DMSO) δ 173.05, 156.09, 155.82, 141.24, 133.78, 131.02 × 2, 129.73, 128.93 × 2, 128.49, 128.20, 127.78 × 2, 126.09, 122.70, 122.06, 117.55, 115.44 × 2, 114.39, 107.17, 32.05, 27.35; HRMS calcd. for $C_{25}H_{19}NO_3$ $[M-H]^-$: 380.1292, found, 380.1296.

2.2. Protein expression and purification

The subcloning and protein expression of human PDE5A1 catalytic domain (residues 535–860) were previously published [42] and are briefly described as follows. The recombinant plasmid of pET15b-PDE5A1 (535–860) was transferred into *E. coli.* strain BL21 (CodonPlus, Stratagene). The *E. coli* cell carrying the pET15-PDE5A1 plasmid was grown in LB medium at 37 °C to absorption A_{600} = 0.6–0.8, and then 0.1 mM isopropyl β-D-thiogalactopyranoside was added to induce the expression at 15 °C for 40 h. The recombinant PDE5A1 protein was purified by column chromatography of Ni-NTA affinity (Qiagen), thrombin cleavage, Q-sepharose ionic exchange, and Sephacryl S200 gel filtration (GE Healthcare). A typical batch of purification yielded 20 mg PDE5A1 from 2-L cell culture. The PDE5A1 protein has purity >95%, as shown by SDS-PAGE.

The catalytic domains of PDE4D2 (86–413), PDE7A1 (130–482), PDE8A2 (480–820), PDE9A2 (181–506), and PDE10A2 (448–789) were purified by using similar protocols previously published [43–47]. PDE1B (1–516) was partially purified (unpublished data).

2.3. Enzymatic assay

The enzymatic activities of the catalytic domains of PDE5A1 and other PDEs were measured by using cGMP or cAMP as substrates and sildenafil and other PDE inhibitors as the reference compounds. The assay buffer contains 50 mM Tris–HCl (pH 8.0), 10 mM $MgCl_2$ or 4 mM $MnCl_2$, 1 mM DTT, 10–30 nM ^{3}H-cGMP or ^{3}H-cAMP (20,000–30,000 cpm/assay, GE Healthcare). The reaction was carried out at room temperature for 15 min and then terminated by addition of 0.2 M $ZnSO_4$. The reaction product ^{3}H-GMP or ^{3}H-AMP was precipitated by 0.2 N $Ba(OH)_2$, while unreacted ^{3}H-cGMP or ^{3}H-cAMP was remained in the supernatant. Radioactivity of the supernatant was measured in 2.5 ml Ultima Gold liquid scintillation cocktails (Fisher Scientific) by a PerkinElmer 2910 liquid scintillation counter. For the measurement of IC_{50}, at least eight concentrations of inhibitors were used in the presence of suitable concentrations of ^{3}H-cAMP/^{3}H-cGMP and the enzymes that hydrolyze up to 70% of the substrates. Each measurement was repeated three times. The IC_{50} values were calculated by nonlinear regression.

2.4. Crystallization and structure determination

The crystals of PDE5A1 were grown by the hanging drop vapor diffusion method. The unliganded PDE5A1 (535–860) (6–10 mg/mL in a storage buffer of 50 mM NaCl, 20 mM Tris–HCl pH 7.5, 1 mM β-mercaptoethanol and 1 mM EDTA) was vapor-diffused against the well buffer of 0.2 M $MgSO_4$, 0.1 M Na cacodylate (pH 6.5), and 18% PEG3350 at room temperature. The crystal size of the unliganded PDE5A1 was improved by micro-seeding against the same crystallization buffer. The PDE5A1-**57** complex was prepared by soaking the unliganded PDE5A1 crystals in the crystallization buffer plus 5 mM **57** at 24 °C for 3 days. The crystals were flash-frozen in liquid nitrogen by using the well buffer plus 20% (w/v) glycerol as the cryosolvent. The X-ray diffraction data were collected at 100 K on Beamline X29 of Brookhaven National Laboratory (Table 3) and processed by HKL2000 [48]. The structure of the PDE5A1-**57** complex was solved by the molecular replacement [49]. The resulted model was rebuilt by program O [50] and refined by CNS [51].

2.5. Docking

The crystal structure of the PDE5A catalytic domain in complex with sildenafil (PDB code 2H42) was used for the virtual docking by the CDOCKER protocol embedded in Accelrys Discovery Studio 2.5.5 [52]. In order to validate the reliability of the default parameters of CDOCKER, the bound sildenafil was docked to the active site of PDE5, yielding the root-mean-squared deviations

(RMSDs) of <1.0 Å for 23 out of total 50 poses from the bound conformation of sildenafil in the crystal. Then, fifty conformations of each designed compound were randomly generated, optimized, and evaluated on the basis of both docking score and cluster population.

The new scaffolds were designed on the basis of the PDE5-**57** crystal structure and docked by program AutoDock 4.2 [53] into the active sites of PDE4D2 (79–413) [43], PDE5A1 (535–860), and PDE9A2 (191–506) [47]. The rigid monomeric PDE catalytic domains were used for docking of all scaffolds. The default docking parameters were verified by docking of **57** into the crystal structure and then used for the scaffold docking. A typical box with 60 × 60 × 60 grid points equally spaced at 0.375 Å per grid was generated using AutoGrid [53]. The following parameters and Lamarckian genetic algorithm were used for the docking: random initial orientation and position, population size (150), maximum number of energy evaluations (25 million), maximum number of generations (27,000), mutation rate (0.02), crossover rate (0.8), and 100 docking runs to output 100 docked conformations.

3. Results

3.1. Structure-based molecular design

We previously reported the synthesis of a series of 1-aryl chromeno[2,3-c]pyrrol-9(2H)-one (ACPs) that may have anticancer activity [41]. Since these compounds contain a chromeno-pyrrol core similar to that of Johnson's PDE5 inhibitors RWJ387273 and RWJ444772 [54,55], we tested their ability to bind to the active site of PDE5. The docking of the ACP compounds to PDE5A shows that some of them occupy the same pocket as sildenafil does, and also are capable of forming a hydrogen bond with invariant Gln817 and π–π stack against conserved Phe820, suggesting that these compounds may be developed to PDE5A inhibitors. Indeed, the enzymatic assay confirmed the inhibitory activity of the compounds on PDE5. Thus, the triple ACP ring was chosen as the pharmacophore and various substitutions on R_1 to R_5 were designed to optimize the inhibition on PDE5 (Table 1).

3.2. Discovery of aryl chromeno-pyrrol analogs as PDE5 inhibitors

The inhibitory activities of obtained aryl chromeno-pyrrol analogs were evaluated by enzymatic assay (Table 1). In summary, most compounds have the IC_{50} values less than 1 μM against PDE5A1, and small substitutions on R_1, R_2, and R_5 (–CH_3, –OCH_3, or –Br) do not dramatically improve the inhibitory activity (compounds **16**–**19**, **22**, **24**, **25**, **35**, **39**, **45**, **47**, **48**, **51**, **53**–**56**, **60**, and **62**). The activity of the compounds largely depends on the substitutions on R_3 and R_4, as discussed as follows.

For substitution on R_3, the small modifications such as the exchanges between furan, thiophen, fluorobenzene, and benzene do not significantly change the IC_{50} values, as shown by the comparisons of **16** vs. **39**, **17** vs. **24**, **21** vs. **26**, **37** vs. **38**, **50** vs. **56**, and **57** vs. **61** (Table 1). However, significant improvement is observed for the cases, in which (1) furan (**19** or **20**) is better than 4-Br-C_6H_4– (**23**) and 4-C_6H_5-C_6H_4– (**49**), and (2) thiophen (**57**) is better than 4-O(CH_3)-C_6H_4– (**58**) or naphthalene (**59**). These data suggest that the compounds with small substitutions on R_3 have better activity than those with large substitutions. This conclusion is also supported by the comparisons of **36** vs. **33** and **61** vs. **59**.

For R_4, substitution with –$CH_2C_6H_4$(*p*-O^{t}Bu) (**23**, **25**, **34**, **43**, and **49**) or –$CH_2(CH_2)_3NHCOO^tBu$ (**41** and **46**–**48**) produces poor inhibition with IC_{50} > 10 μM, while the –$CH_2CH_2COO^tBu$ substitution yields IC_{50} in a range 0.8–4 μM (**17**, **18**, **21**, **22**, **24**, and **26**, Table 1). The –CH_2COO^tBu substitution results in the moderate inhibitors of **16**, **35**, **37**, **38**, and **39** with IC_{50} = 446, 122, 381, 217, and 492 nM, respectively. Thus, the above data suggest that a smaller group linked to O^{t}Bu have better inhibitory activity, and also imply that the *t*-butanyl group may be a steric obstacle for interaction with PDE5 so as to scarify the inhibition. The best substitution on R_4 is –$CH_2C_6H_4$(*p*-OH), and compounds containing this substitution showed the IC_{50} values of 456 (**59**), 356 (**53**), 221 (**58**), 137 (**62**), 135 (**55**), 61 (**51**), 18 (**61**), and 17 nM (**57**), respectively.

In summary, four compounds **42**, **51**, **57**, and **61** show the potent IC_{50} values of 77, 61, 17, and 18 nM, and may thus be deserved for further pharmacological studies. Compound **57** was selected for more complete assay and shows reasonably good selectivity over the catalytic domains of the other PDE families (Table 2).

3.3. Architecture of the PDE5-57 structure

The crystallographic asymmetric unit contains one PDE5 catalytic domain in complex with **57**. The structure of the PDE5-**57** complex (Fig. 2) has the overall similar folding as those of other PDE5 catalytic domains [42,56–62], as shown by the average positional differences of 0.24 and 0.26 Å for 286 and 279 comparable Cα atoms when PDE5-**57** was superimposed over the structures of the unliganded PDE5 and its complex with sildenafil [42]. A significant portion of the H-loop (667–676) and the M-loop (791–807) is disordered in the PDE5-**57** complex. This is similar to the disorder of the H-loop in the structures of the unliganded PDE5 and its IBMX complex [42,61], but different from the ordered conformation of the H-loops in the PDE5 complexes with sildenafil and vardenafil, in which the H-loops showed large positional migrations and different conformations [42,59].

3.4. Binding of inhibitor 57

Inhibitor **57** binds to the active site of PDE5 as other PDE5 inhibitors do (Fig. 2). The aryl-chromeno-pyrrol ring of **57** is sandwiched by the hydrophobic residues of Phe820 on one side and Val782 and Phe786 on another side (Fig. 2B and C). In addition, the amine on the pyrrol ring of **57** forms a hydrogen bond with the amide oxygen of the Gln817 side chain of PDE5 (2.5 Å). This hydrogen bond with Gln817 and the stack against Phe820 are two characteristics conserved for the binding of many PDE inhibitors [62]. The tyrosyl group of **57** interacts with hydrophobic residues of Val782, Ala783, Phe787, Ile813, and Met816, although the docking suggested that its OH group may form a hydrogen bond with the carbonyl oxygen of Leu804 that is disordered in the crystal. The thiophen ring of **57** forms a hydrogen bond with the amide nitrogen of Gln817 (3.3 Å to the sulfur), in addition to the hydrophobic interactions with residues of Ala767, Ile768, Gln775, and Ile778.

The electron density maps of (2Fo – Fc) and (Fo – Fc) unambiguously revealed the conformation of **57**, in which the thiophen ring conjugated with the aryl-chromeno-pyrrol plane, but tilted slightly (Fig. 2C). However, the B-factor of **57** (86 $Å^2$) is significantly higher than the average B-factor of the protein atoms (48 $Å^2$, Table 3), suggesting its low occupancy. A possible explanation to the low occupancy of **57** might be the unfavorable match of the polar chromenol ring with the hydrophobic residues Phe820, Val782, and Phe786 (Fig. 2B and C). Another possibility might be the close contact of a carbon atom on the aryl ring of **57** with an oxygen of the bound sulfate group in a hydrogen bond distance. The sulfate group is not an integrated part of the protein, but may be recruited from the crystallization buffer containing 0.2 M $MgSO_4$. The sulfate replaced a chelating water of the zinc ion and its occupancy at the active site is supported by its comparable

Table 1
Structures of ACPs and their IC_{50} values (nM) for PDE5A1.

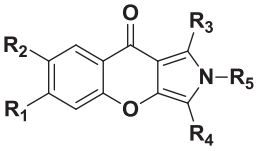

Cpd.	R_1	R_2	R_3	R_4	R_5	$IC_{50} \pm SD$[a]
16	H	CH_3	Furan-2-yl	CH_2COO^tBu	H	446 ± 6
17	H	OCH_3	Furan-2-yl	$CH_2CH_2COO^tBu$	H	4379 ± 450
18	H	CH_3	Furan-2-yl	$CH_2CH_2COO^tBu$	H	1667 ± 80
19	H	CH_3	Furan-2-yl	$CH_2C_6H_4$(*p*-O^tBu)	H	240 ± 44
20	H	H	Furan-2-yl	$CH_2C_6H_4$(*p*-O^tBu)	H	1997 ± 315
21	H	H	Furan-2-yl	$CH_2CH_2COO^tBu$	H	2071 ± 213
22	H	Br	Furan-2-yl	$CH_2CH_2COO^tBu$	H	823 ± 246
23	H	H	4-Br-C_6H_4	$CH_2C_6H_4$(*p*-O^tBu)	H	>10,000 (26%)
24	H	OCH_3	Thiophen-2-yl	$CH_2CH_2COO^tBu$	H	1913 ± 60
25	H	OCH_3	Thiophen-2-yl	$CH_2C_6H_4$(*p*-O^tBu)	H	~10,000
26	H	H	C_6H_5	$CH_2CH_2COO^tBu$	H	2142 ± 290
33	H	H	Naphthalen-2-yl	$CH_2C_6H_5$	H	>10,000 (28%)
34	H	H	Naphthalen-2-yl	$CH_2C_6H_4$(*p*-O^tBu)	H	>10,000 (3%)
35	H	OCH_3	Thiophen-2-yl	CH_2COO^tBu	H	122 ± 27
36	H	H	4-Br-C_6H_4	$CH_2C_6H_5$	H	319 ± 78
37	H	H	C_6H_5	CH_2COO^tBu	H	381 ± 61
38	H	H	4-F-C_6H_4	CH_2COO^tBu	H	217 ± 25
39	H	CH_3	4-F-C_6H_4	CH_2COO^tBu	H	492 ± 35
40	H	H	4-F-C_6H_4	N-Boc-1*H*-indol-3-yl	H	>10,000 (21%)
41	H	H	C_6H_5	$CH_2(CH_2)_3NHCOO^tBu$	H	~10,000
42	H	H	C_6H_5	$CH_2C_6H_5$	H	77 ± 11
43	H	H	C_6H_5	$CH_2C_6H_4$(*p*-O^tBu)	H	>10,000 (40%)
44	OCH_3	H	Thiophen-2-yl	$CH_2CH(CH_3)_2$	H	836 ± 17
45	H	CH_3	Furan-2-yl	$CH_2CH(CH3)_2$	H	576 ± 7
46	OCH_3	H	Thiophen-2-yl	$CH_2(CH_2)_3NHCOO^tBu$	H	~10,000
47	H	CH_3	Thiophen-2-yl	$CH_2(CH_2)_3NHCOO^tBu$	H	>10,000 (41%)
48	H	OCH_3	Thiophen-2-yl	$CH_2(CH_2)_3NHCOO^tBu$	H	2463 ± 426
49	H	H	4-C_6H_5-C_6H_4	$CH_2C_6H_4$(*p*-O^tBu)	H	>10,000 (6%)
50	H	OCH_3	Thiophen-2-yl	CH_2CH_2COOH	H	4166 ± 76
51	H	OCH_3	Thiophen-2-yl	$CH_2C_6H_4$(*p*-OH)	H	61 ± 3
52	H	H	C_6H_5	CH_2CH_2COOH	H	~10,000
53	H	CH_3	4-F-C_6H_4	$CH_2C_6H_4$(*p*-OH)	H	356 ± 34
54	H	Br	Thiophen-2-yl	CH_2CH_2COOH	H	2818 ± 370
55	H	Br	Thiophen-2-yl	$CH_2C_6H_4$(*p*-OH)	H	135 ± 17
56	H	CH_3	4-F-C_6H_4	CH_2CH_2COOH	H	4626 ± 725
57	H	H	Thiophen-2-yl	$CH_2C_6H_4$(*p*-OH)	H	17 ± 1
58	H	H	4-OCH_3-C_6H_4	$CH_2C_6H_4$(*p*-OH)	H	221 ± 3
59	H	H	Naphthalen-2-yl	$CH_2C_6H_4$(*p*-OH)	H	456 ± 24
60	H	H	C_6H_5	$CH_2C_6H_5$	CH_3	902 ± 31
61	H	H	C_6H_5	$CH_2C_6H_4$(*p*-OH)	H	18 ± 4
62	H	H	C_6H_5	$CH_2C_6H_4$(*p*-OH)	CH_3	137 ± 16

[a] The percentiles in parentheses indicate the inhibitory rate at 10,000 nM of the inhibitors.

B-factor (35 $Å^2$) with the overall B-factor for protein atoms (48 $Å^2$) from the structural refinement (Table 3). The last possibility might be due to the fact that **57** does not fit well to the pocket of the unliganded PDE5 by the soaking experiments since at least 6 conformations of the H-loop at the active site of PDE5 have been identified [42,59–62].

The structural information is ready for explanation of the activity data. The attachment of a methyl group to R5 of **57** would abolish the hydrogen bond between the nitrogen of pyrrol of **57** and Gln817 (Fig. 2) and thus scarify the potency of the inhibitors **60** and **62** (Table 1). The contact of thiophen with the hydrophobic residues of Ala767, Ile768, Ile778, and Phe820, may explain the observation that the benzyl replacement produced an inhibitor with a similar IC_{50} (18 nM for **61**, Table 1). The dead end location of the thiophen ring of **57** in PDE5 would predict that a large substitution at R3 results in poor inhibitors, and this indeed happens to compounds **33** and **34** ($IC_{50} > 10$ μM, Table 1). The fit of the tyrosyl ring of **57** to the hydrophobic environment in the crystal structure might explain that the compounds containing a polar ester group at R4 (**16–18**, **21**, **22**, **24**, **26**, **37–39**, **41**, **46–48**, **50**, **52**, **54**, and **56**) would not be highly potent inhibitors due to its polarity or steric hindrance.

3.5. Similarities and differences of 57 binding from those of other PDE5 inhibitors

Superposition of PDE5-**57** over the other PDE5-inhibitor structures [42,56–62] reveals an overall similar binding between

Table 2
Enzymatic activity of **57** (IC_{50}, μM) against catalytic domains of PDEs.

PDEs	1B2 (10–487)	4D2 (86–413)	5A1 (535–860)	7A1 (130–482)	8A1 (480–820)	9A2 (181–506)	10A2 (447–789)
57	2.00 ± 0.27	1.45 ± 0.11	0.017 ± 0.001	0.99 ± 0.06	2.76 ± 0.73	11.68 ± 0.16	0.75 ± 0.19

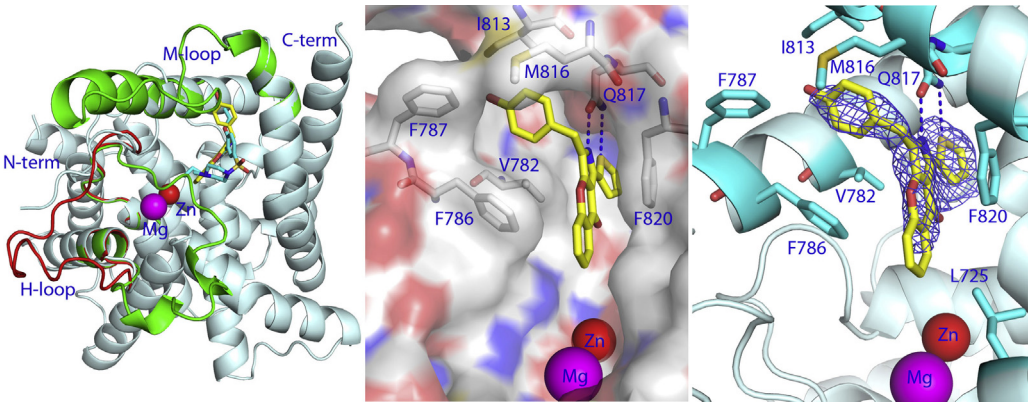

Fig. 2. Structure of the PDE5-**57** complex. (A) Ribbon presentation of the PDE5 catalytic domain (cyan ribbons) in complex with **57** (yellow stick). The red and green ribbons show the conformations of the H- and M-loops of the unliganded PDE5 and its complex with sildenafil, respectively. The comparable portions of the three structures are represented by the cyan ribbons. (B) Surface model for the **57** (yellow sticks) binding. The dotted lines represent hydrogen bonds. (C) Interaction of **57** with PDE5. The blue mesh is the electron density map of (Fo − Fc) that was calculated from the structure with omission of **57** and contoured at 2.5σ. (For interpretation of the references to color in this figure legend, the reader is referred to the web version of the article.)

57 and other PDE5 inhibitors, but different interactions in detail. When **57** is compared with sildenafil and tadalafil, the binding of **57** to PDE5 shows a pattern closer to that of tadalafil than sildenafil (Fig. 3). The interactions of the triple ACP ring of **57** with conserved Phe820 and invariant Gln817 are closely simulated by the stack of pyrazolo-pyrimidine ring of sildenafil against Phe820 and two hydrogen bonds with Gln817 in the PDE5-sildenafil structure [42]. However, the ethoxy group of sildenafil makes much less contribution to the hydrophobic interactions with a small pocket made up of Phe787, Ile813, and Met816, than the tyrosyl group of **57** in the PDE5-**57** structure, although they occupy the same location (Fig. 3). Besides, sulfonyl-4-methylpiperazine of sildenafil and pyrrol of **57** occupy different locations and interact with different residues.

In comparison, the chromeno-pyrrol and thiophen rings of **57** are well superimposed over the four conjugated ring of pyrazino-pyrido-indole of tadalafil (Fig. 3). These rings in the structures of PDE5-tadalafil and PDE5-**57** commonly fit to the hydrophobic slot made up of Val782, Phe786, and Phe820, and form a hydrogen bond with invariant Gln817. The tyrosyl ring of **57** and benzodioxol ring of tadalafil occupy the same hydrophobic pocket consisted of Phe787, Ile813, and Met816, although their detailed interactions are not exactly comparable (Fig. 3). However, Gln817 forms only one hydrogen bond with the amine on the indole ring of tadalafil, in comparison to two hydrogen bonds with the pyrrol amine and thiophen sulfur of **57**.

Table 3
Statistics on diffraction data and structure refinement.

Data collection	PDE5-**57**
Space group	$P3_121$
Unit cell (*a*, *c*, Å)	74.1, 132.3
Resolution (Å)	50–2.0 (2.07–2.0)
Total measurements	666,527
Unique reflections	29,180
Completeness (%)	100.0 (100.0)
Average I/σ	14.0 (5.2)
R_{merge}	0.065 (0.688)
Structure refinement	
R-factor/R-free	0.217/0.248
Reflections	28,434/2830
Resolution (Å)	15–2.0
RMS deviations for	
Bond length	0.0052 Å
Bond angle	1.1°
Average B-factor (Å^2) (atoms)	
Protein 47.5 (2420)	
Inhibitor	85.6 (23)
Zn	38.3 (1)
Mg	41.8 (1)
SO_4	35.0 (5)
Water	44.0 (75)
Ramachandran plot	
Most favored	91.0%
Allowed	7.9%
General allowed	1.1%

4. Discussion

4.1. Implication on a new scaffold for development of PDE inhibitors

While the enzymatic and structural studies have shown that **57** is a PDE5 selective inhibitor, its potency may be further improved. For example, replacement of the triple ACP ring of **57** with a small ring system may avoid of the unfavorable interactions of the hydrophobic aryl group with the hydrophilic solvent molecules at the metal binding pocket. Another possible modification is replacement of the polar chromeno group of **57** with a hydrophobic ring in order to favorably fit to the hydrophobic slot of PDE5, which is composed of Phe820, Val782, Phe786, and Phe787.

On the other hand, since **57** has a different chemical skeleton from other PDE5 inhibitors (Fig. 1), a fragment of our inhibitors might be taken as a scaffold for development of PDE inhibitors. An example of the scaffolds may be methoxyl-phenyl-pyrrol-thiophen (**5R3**, Fig. 1). The docking of **5R3** into the catalytic domains of cGMP-specific PDE5A1 and PDE9A2, and cAMP-specific PDE4D2 shows that **5R3** binds to the PDEs with the predicted K_i values at micromolar level. The best poses from the dockings showed the similar interactions of **5R3** with PDE5 and PDE9, such as stacking against the conserved phenylalanine and hydrogen-bonding with the invariant glutamine (Fig. 4). Thus, **5R3** could be used as a scaffold that has the basic binding affinity with PDE5 and PDE9 while the selectivity may be achieved by targeting at non-conserved residues in the PDE5 and PDE9 pockets. On the other hand, **5R3** binding to cAMP-specific PDE4 is completely different from those of cGMP-specific PDE5 and PDE9 (Fig. 4C). While the stack against the phenylalanine (Phe372 in PDE4D2) is still conserved, the pyrrol amine of **5R3** forms a hydrogen bond with Asn321, instead of the invariant glutamine (Gln369 in PDE4D2). In short, on the basis of the different binding patterns, **5R3** might be redesigned to lead to inhibitors for various PDE families.

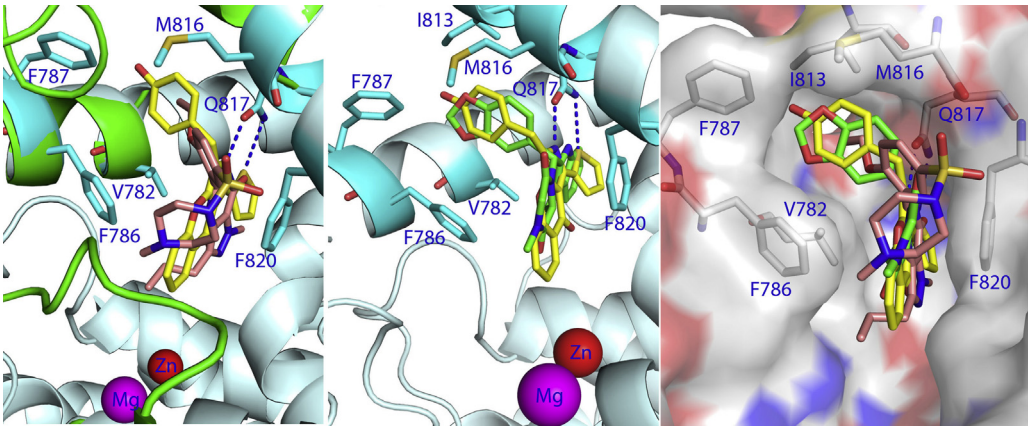

Fig. 3. Comparison on binding of the PDE5 inhibitors. (A) Superposition of the PDE5-**57** complex (cyan ribbons and yellow sticks) over the PDE5-sildenafil structure (green ribbons and salmon sticks). (B) Comparison on the binding of **57** (yellow sticks) and tadalafil (green). Since the PDE5-tadalafil structure (PDB code 1XOZ) contains a replacement of the H-loop with the PDE4 fragment, no comparison on the protein structures is shown. (C) Surface model on the binding of inhibitors of **57** (yellow), sildenafil (salmon), and tadalafil (green). (For interpretation of the references to color in this figure legend, the reader is referred to the web version of the article.)

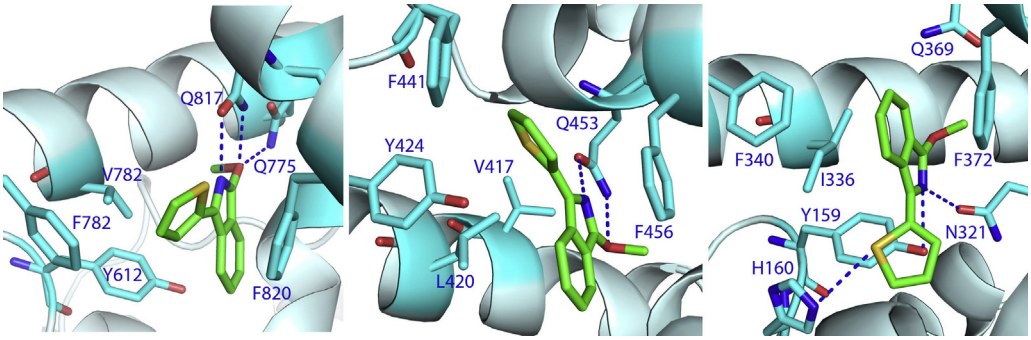

Fig. 4. Docking of a new scaffold **5R3** to cGMP-specific PDE5A1 (A) and PDE9A2 (B), and cAMP-specific PDE4D2 (C). Dotted lines represent hydrogen bonds. It is visible that the scaffold **5R3** binds to the PDEs in different orientations and has different patterns of hydrogen bonding in the structures of PDE4, PDE5, and PDE9, but the stacking against the conserved phenylalanine is retained. (For interpretation of the references to color in this figure legend, the reader is referred to the web version of the article.)

Acknowledgments

We thank Dr. Howard Robinson at Brookhaven National Laboratory for help with collection of the diffraction data. This work is partially supported by US NIH GM59791 (H. Ke), Natural Science Foundation of China (30973619, 81172931, 21103234, and 81373258), Guangdong Natural Science Foundation (S2011030003190), Guangdong Science Foundation (2012A080201007), Guangdong Provincial Key Laboratory of Construction Foundation (2011A060901014), and Fundamental Research Funds for the Central Universities (11ykzd05 and 09ykpy66).

References

[1] Bender AT, Beavo JA. Cyclic nucleotide phosphodiesterases: molecular regulation to clinical use. Pharmacol Rev 2006;58:488–520.
[2] Omori K, Kotera J. Overview of PDEs and their regulation. Circ Res 2007;100:309–27.
[3] Conti M, Beavo JA. Biochemistry and physiology of cyclic nucleotide phosphodiesterases: essential components in cyclic nucleotide signaling. Annu Rev Biochem 2007;76:481–511.
[4] De Felice FG, Wasilewska-Sampaio AP, Barbosa AC, Gomes FC, Klein WL, Ferreira ST, et al. Cyclic AMP enhancers and Abeta oligomerization blockers as potential therapeutic agents in Alzheimer's disease. Curr Alzheimer Res 2007;4:263–71.
[5] Jarnaess E, Taskén K. Spatiotemporal control of cAMP signalling processes by anchored signalling complexes. Biochem Soc Trans 2007;35:931–7.
[6] Jin XL, O'Neill C. cAMP-responsive element-binding protein expression and regulation in the mouse preimplantation embryo. Reproduction 2007;134:667–75.
[7] Piper M, van Horck F, Holt C. The role of cyclic nucleotides in axon guidance. Adv Exp Med Biol 2007;621:134–43.
[8] Zaccolo M, Movsesian MA. cAMP and cGMP signaling crosstalk: role of phosphodiesterases and implications for cardiac pathophysiology. Circ Res 2007;100:1569–78.
[9] Galie N, Ghofrani HA, Torbicki A, Barst RJ, Rubin LJ, Badesch D, et al. Sildenafil citrate therapy for pulmonary arterial hypertension. N Engl J Med 2005;353:2148–57.
[10] Blokland A, Schreiber R, Prickaerts J. Improving memory: a role for phosphodiesterases. Curr Pharm Des 2006;12:2511–23.
[11] Menniti FS, Faraci WS, Schmidt CJ. Phosphodiesterases in the CNS: targets for drug development. Nat Rev Drug Discov 2006;5:660–70.
[12] Miller CL, Oikawa M, Cai Y, Wojtovich AP, Nagel DJ, Xu X, et al. Role of Ca^{2+}/calmodulin-stimulated cyclic nucleotide phosphodiesterase 1 in mediating cardiomyocyte hypertrophy. Circ Res 2009;105:956–64.
[13] Hutson PH, Finger EN, Magliaro BC, Smith SM, Converso A, Sanderson PE, et al. The selective phosphodiesterase 9 (PDE9) inhibitor PF-04447943 (6-[(3S,4S)-4-methyl-1-(pyrimidin-2-ylmethyl)pyrrolidin-3-yl]-1-(tetrahydro-2H-pyran-4-yl)-1,5-dihydro-4H-pyrazolo[3,4-d] pyrimidin-4-one) enhances synaptic plasticity and cognitive function in rodents. Neuropharmacology 2011;61:665–76.
[14] Reid DJ, Pham NT. Roflumilast: a novel treatment for chronic obstructive pulmonary disease. Ann Pharmacother 2012;46:521–9.
[15] Rotella DP. Phosphodiesterase 5 inhibitors: current status and potential applications. Nat Rev Drug Discov 2002;1:674–82.
[16] Keating GM, Scott LJ. Vardenafil: a review of its use in erectile dysfunction. Drugs 2003;63:2673–703.
[17] Kotera J, Mochida H, Inoue H, Noto T, Fujishige K, Sasaki T, et al. Avanafil: a potent and highly selective phosphodiesterase-5 inhibitor for erectile dysfunction. J Urol 2012;188:668–74.
[18] Oh TY, Kang KK, Ahn BO, Yoo M, Kim WB. Erectogenic effect of the selective phosphodiesterase type 5 inhibitor. DA-8159. Arch Pharm Res (NY) 2000;23:471–6.
[19] Jung JY, Kim SK, Kim BS, Lee SH, Park YS, Kim SJ, et al. The penile erection efficacy of a new phosphodiesterase type 5 inhibitor, mirodenafil (SK3530), in rabbits with acute spinal cord injury. J Vet Med Sci 2008;70:1199–204.

[20] Udeoji DU, Schwarz ER. Tadalafil as monotherapy and in combination regimens for the treatment of pulmonary arterial hypertension. Ther Adv Respir Dis 2013;7:39–49.
[21] Andersson KE, de Groat WC, McVary KT, Lue TF, Maggi M, Roehrborn CG, et al. Tadalafil for the treatment of lower urinary tract symptoms secondary to benign prostatic hyperplasia: pathophysiology and mechanism(s) of action. Neurourol Urodyn 2011;30:292–301.
[22] Mouli S, McVary KT. PDE5 inhibitors for LUTS. Prostate Cancer Prostatic Dis 2009;12:316–24.
[23] Miller MS. Role of phosphodiesterase type 5 inhibitors for lower urinary tract symptoms. Ann Pharmacother 2013;47:278–83.
[24] Kass DA, Champion HC, Beavo JA. Phosphodiesterase type 5: expanding roles in cardiovascular regulation. Circ Res 2007;101:1084–95.
[25] Kukreja RC, Salloum FN, Das A. Cyclic guanosine monophosphate signaling and phosphodiesterase-5 inhibitors in cardioprotection. J Am Coll Cardiol 2012;59:1921–7.
[26] Schwartz BG, Levine LA, Comstock G, Stecher VJ, Kloner RA. Cardiac uses of phosphodiesterase-5 inhibitors. J Am Coll Cardiol 2012;59:9–15.
[27] Schwartz BG, Jackson G, Stecher VJ, Campoli-Richards DM, Kloner RA. Phosphodiesterase type 5 inhibitors improve endothelial function and may benefit cardiovascular conditions. Am J Med 2013;126:192–9.
[28] Guazzi M, Samaja M, Arena R, Vicenzi M, Guazzi MD. Long-term use of sildenafil in the therapeutic management of heart failure. J Am Coll Cardiol 2007;50:2136–44.
[29] Cvelich RG, Roberts SC, Brown JN. Phosphodiesterase type 5 inhibitors as adjunctive therapy in the management of systolic heart failure. Ann Pharmacother 2011;45:1551–8.
[30] Kanwar M, Agarwal R, Barnes M, Coons J, Raina A, Sokos G, et al. Role of phosphodiesterase-5 inhibitors in heart failure: emerging data and concepts. Curr Heart Fail Rep 2013;10:26–35.
[31] Roustit M, Blaise S, Allanore Y, Carpentier PH, Caglayan E, Cracowski JL. Phosphodiesterase-5 inhibitors for the treatment of secondary Raynaud's phenomenon: systematic review and meta-analysis of randomised trials. Ann Rheum Dis 2013;72:1696–9.
[32] Percival JM, Adamo CM, Beavo JA, Froehner SC. Evaluation of the therapeutic utility of phosphodiesterase 5A inhibition in the mdx mouse model of duchenne muscular dystrophy. Handb Exp Pharmacol 2011;204:323–44.
[33] Gonzalez-Cadavid NF, Rajfer J. Treatment of Peyronie's disease with PDE5 inhibitors: an antifibrotic strategy. Nat Rev Urol 2010;7:215–21.
[34] Puzzo D, Sapienza S, Arancio O, Palmeri A. Role of phosphodiesterase 5 in synaptic plasticity and memory. Neuropsychiatr Dis Treat 2008;4:371–87.
[35] Rondina MT, Weyrich AS. Targeting phosphodiesterases in anti-platelet therapy. Handb Exp Pharmacol 2012;210:225–38.
[36] Farsaie S, Khalili H, Karimzadeh I, Dashti-Khavidaki S. An old drug for a new application: potential benefits of sildenafil in wound healing. J Pharm Pharm Sci 2012;15:483–98.
[37] Schmidt CJ. Phosphodiesterase inhibitors as potential cognition enhancing agents. Curr Top Med Chem 2010;10:222–30.
[38] Dimitriadis F, Giannakis D, Pardalidis N, Zikopoulos K, Paraskevaidis E, Giotitsas N, et al. Effects of phosphodiesterase-5 inhibitors on sperm parameters and fertilizing capacity. Asian J Androl 2008;10:115–33.
[39] Azzouni F, Abu samra K. Are phosphodiesterase type 5 inhibitors associated with vision-threatening adverse events? A critical analysis and review of the literature. J Sex Med 2011;8:2894–903.
[40] Khan AS, Sheikh Z, Khan S, Dwivedi R, Benjamin E. Viagra deafness—sensorineural hearing loss and phosphodiesterase-5 inhibitors. Laryngoscope 2011;121:1049–54.
[41] Yu Y, Hu Y, Shao W, Huang J, Zuo Y, Huo Y, et al. Synthesis of multifunctionalized chromeno[2,3-c]pyrrol-9(2H)-ones: investigation and application of Baker–Venkataraman rearrangement involved reactions catalyzed by 4-(dimethylamino)pyridine. Eur J Org Chem 2011;24:4551–63.
[42] Wang H, Liu Y, Huai Q, Cai JW, Zoraghi R, Francis SH, et al. Multiple conformations of phosphodiesterase-5: implications for enzyme function and drug development. J Biol Chem 2006;281:21469–79.
[43] Huai Q, Wang H, Sun Y, Kim HY, Liu Y, Ke H. Three dimensional structures of PDE4D in complex with rolipram and implication on inhibitor selectivity. Structure 2003;11:865–73.
[44] Wang H, Liu Y, Chen Y, Robinson H, Ke H. Multiple elements jointly determine inhibitor selectivity of cyclic nucleotide phosphodiesterases 4 and 7. J Biol Chem 2007;280:30949–55.
[45] Wang H, Liu Y, Hou J, Zheng M, Robinson H, Ke H. Structural insight into substrate specificity of phospodiesterase 10. Proc Natl Acad Sci USA 2007;104:5782–7.
[46] Wang H, Yan Z, Yang S, Cai J, Robinson H, Ke H. Kinetic and structural studies of phosphodiesterase-8A and implication on the inhibitor selectivity. Biochemistry 2008;47:12760–68.
[47] Meng F, Hou J, Shao YX, Wu PY, Huang M, Zhu X, et al. Structure-based discovery of highly selective phosphodiesterase-9A inhibitors and implications for inhibitor design. J Med Chem 2012;55:8549–58.
[48] Otwinowski Z, Minor W. Processing of X-ray diffraction data collected in oscillation mode. Methods Enzymol 1997;276:307–26.
[49] Navaza J, Saludjian P. AMoRe: an automated molecular replacement program package. Methods Enzymol 1997;276:581–94.
[50] Jones TA, Zou J-Y, Cowan SW, Kjeldgaard M. Improved methods for building protein models in electron density maps and the location of errors in these models. Acta Cryst 1991;A47:110–9.
[51] Brünger AT, Adams PD, Clore GM, DeLano WL, Gros P, Grosse-Kunstleve RW, et al. Crystallography & NMR system: a new software suite for macromolecular structure determination. Acta Cryst 1998;D54:905–21.
[52] Wu G, Robertson DH, Brooks CL, Vieth M. Detailed analysis of grid-based molecular docking: a case study of CDOCKER—a CHARMm-based MD docking algorithm. J Comput Chem 2003;24:1549–62.
[53] Huey R, Morris GM, Olson AJ, Goodsell DS. Asemiempirical free energy force field with charge-based desolvation. J Comput Chem 2007;28:1145–52.
[54] Jiang W, Guan J, Macielag MJ, Zhang S, Qiu Y, Kraft P, et al. Pyrroloquinolone PDE5 inhibitors with improved pharmaceutical profiles for clinical studies on erectile dysfunction. J Med Chem 2005;48:2126–33.
[55] Lanter JC, Sui Z, Macielag MJ, Fiordeliso JJ, Jiang W, Qiu Y, et al. Structure–activity relationships of N-acyl pyrroloquinolone PDE-5 inhibitors. J Med Chem 2004;47:656–62.
[56] Sung BJ, Hwang KY, Jeon YH, Lee JI, Heo YS, Kim JH, et al. Structure of the catalytic domain of human phosphodiesterase 5 with bound drug molecules. Nature 2003;425:98–102.
[57] Zhang KY, Card GL, Suzuki Y, Artis DR, Fong D, Gillette S, et al. A glutamine switch mechanism for nucleotide selectivity by phosphodiesterases. Mol Cell 2004;15:279–86.
[58] Card GL, England BP, Suzuki Y, Fong D, Powell B, Lee B, et al. Structural basis for the activity of drugs that inhibit phosphodiesterases. Structure 2004;12:2233–47.
[59] Wang H, Ye M, Robinson H, Francis SH, Ke H. Conformational variations of both PDE5 and inhibitors provide the structural basis for the physiological effects of vardenafil and sildenafil. Mol Pharmacol 2008;73:104–10.
[60] Chen G, Wang H, Robinson H, Cai J, Wan Y, Ke H. An insight into the pharmacophores of phosphodiesterase-5 inhibitors from synthetic and crystal structural studies. Biochem Pharmacol 2008;75:1717–28.
[61] Huai Q, Liu Y, Francis SH, Corbin JD, Ke H. Crystal structures of phosphodiesterases 4 and 5 in complex with inhibitor IBMX suggest a conformation determinant of inhibitor selectivity. J Biol Chem 2004;279:13095–101.
[62] Ke H, Wang H. Crystal structures of phosphodiesterases and implications on substrate specificity and inhibitor selectivity. Curr Top Med Chem 2007;7:391–403.